Mitochondrial function in the brain links anxiety with social subordination

Fiona Hollis[a,1], Michael A. van der Kooij[a,1,2], Olivia Zanoletti[a], Laura Lozano[a], Carles Cantó[b], and Carmen Sandi[a,3]

[a]Brain Mind Institute, École Polytechnique Fédérale de Lausanne, CH-1015 Lausanne, Switzerland; and [b]Nestlé Institute of Health Sciences SA, CH-1015 Lausanne, Switzerland

Edited by Bruce S. McEwen, The Rockefeller University, New York, NY, and approved October 29, 2015 (received for review June 27, 2015)

Dominance hierarchies are integral aspects of social groups, yet whether personality traits may predispose individuals to a particular rank remains unclear. Here we show that trait anxiety directly influences social dominance in male outbred rats and identify an important mediating role for mitochondrial function in the nucleus accumbens. High-anxious animals that are prone to become subordinate during a social encounter with a low-anxious rat exhibit reduced mitochondrial complex I and II proteins and respiratory capacity as well as decreased ATP and increased ROS production in the nucleus accumbens. A causal link for these findings is indicated by pharmacological approaches. In a dyadic contest between anxiety-matched animals, microinfusion of specific mitochondrial complex I or II inhibitors into the nucleus accumbens reduced social rank, mimicking the low probability to become dominant observed in high-anxious animals. Conversely, intraaccumbal infusion of nicotinamide, an amide form of vitamin B3 known to enhance brain energy metabolism, prevented the development of a subordinate status in high-anxious individuals. We conclude that mitochondrial function in the nucleus accumbens is crucial for social hierarchy establishment and is critically involved in the low social competitiveness associated with high anxiety. Our findings highlight a key role for brain energy metabolism in social behavior and point to mitochondrial function in the nucleus accumbens as a potential marker and avenue of treatment for anxiety-related social disorders.

anxiety | mitochondria | nucleus accumbens | social dominance | social competition

In most socially living species, the social rank of an individual is established during competitive encounters with conspecifics. The outcome of these encounters determines the allocation of territory, resources and access to reproduction (1), and greatly influences physiology and health (2). Winning a social competition is rewarding, enhances rank in social hierarchies, and increases the probability of winning future contests (3, 4). In contrast, losing a social encounter typically undermines one's social rank. In humans, a low social status predicts morbidity and survival (5) and has also been linked to the development of psychopathologies (6). Despite the important consequences of social rank on health, little is known regarding the mechanisms underlying the establishment of social hierarchies.

One of the main reasons for the paucity of neurobiological mechanisms determining social hierarchies may be that social competition involves interacting subjects that both need to be taken into account. The competitors may exhibit different features such as size, age, gender, as well as previous social experience, all known to influence social competitiveness. However, when subjects are matched for these characteristics, the impact of innate personality traits on social competitiveness may be investigated. One such personality trait, anxiety, may have important consequences for the outcome of social competitions. In humans, high-anxious individuals often display a subordinate status and report feelings of being overlooked and rejected (7), and their competitive self-confidence becomes undermined under stress (8). Thus, interindividual differences in anxiety could predetermine the outcome of a competitive encounter and, as such, trait anxiety may have important consequences for social status. However, the neural mechanisms whereby anxiety might affect social hierarchy formation are largely unknown.

We addressed this question by examining social competitiveness between male rats characterized for trait anxiety. Recent work has highlighted the potential for individual differences in mitochondrial function and, more broadly, energy metabolism to influence vulnerability to develop psychopathological disorders, such as anxiety and depression (9–14). Here, we demonstrate that trait anxiety is a determining factor of social rank that is mediated by brain region-specific mitochondrial function. We show that manipulation of mitochondrial function in the nucleus accumbens (NAc) is sufficient to influence social rank, highlighting a key role for brain mitochondrial function in social behavior.

Results

High Trait Anxiety Is a Predisposing Factor to Social Subordination. To establish the relationship between anxiety and the outcome of a social competition, male outbred rats were first classified as high-, intermediate-, or low-anxious based on natural variation for anxiety-like behavior on the elevated plus maze (Fig. 1 *A*–*C* and *SI Appendix*, Fig. S1*A*). Their anxiety profiles were confirmed in another validated test for anxiety, the light–dark box (Fig. 1 *D* and *E* and *SI Appendix*, Fig. S1 *B*–*D*). Then, high-anxious and low-anxious rats were matched for body weight, age, and social experience, and allowed to compete for a new territory. High-anxious rats exhibited reduced offensive behavior during the social encounter (Fig. 1*F* and

Significance

Within a dominance hierarchy, low social status strongly reduces individual well-being. In socially living species, rank in a hierarchy is determined through competitive encounters. Despite the numerous health consequences, the ability of personality traits to predispose individuals to a particular social rank remains largely unclear. Our work identifies trait anxiety as a predisposing factor to a subordinate rank. We demonstrate that mitochondrial function in the nucleus accumbens, a brain region relevant for motivation and depression, is a critical mediating factor in the subordinate status displayed by high-anxious rats. These findings highlight a role for cerebral energy metabolism in social behavior and point to mitochondrial function in the nucleus accumbens as a potential marker and avenue of treatment for mood disorders.

Author contributions: F.H., M.A.v.d.K., C.C., and C.S. designed research; F.H., M.A.v.d.K., O.Z., L.L., and C.C. performed research; F.H., M.A.v.d.K., and C.S. analyzed data; and F.H., M.A.v.d.K., C.C., and C.S. wrote the paper.

The authors declare no conflict of interest.

This article is a PNAS Direct Submission.

Freely available online through the PNAS open access option.

[1]F.H. and M.A.v.d.K. contributed equally to this work.

[2]Present address: Johannes Gutenberg University Medical Centre, Department of Psychiatry and Psychotherapy and Focus Program, Translational Neurosciences, 55128 Mainz, Germany.

[3]To whom correspondence should be addressed. Email: carmen.sandi@epfl.ch.

This article contains supporting information online at www.pnas.org/lookup/suppl/doi:10.1073/pnas.1512653112/-/DCSupplemental.

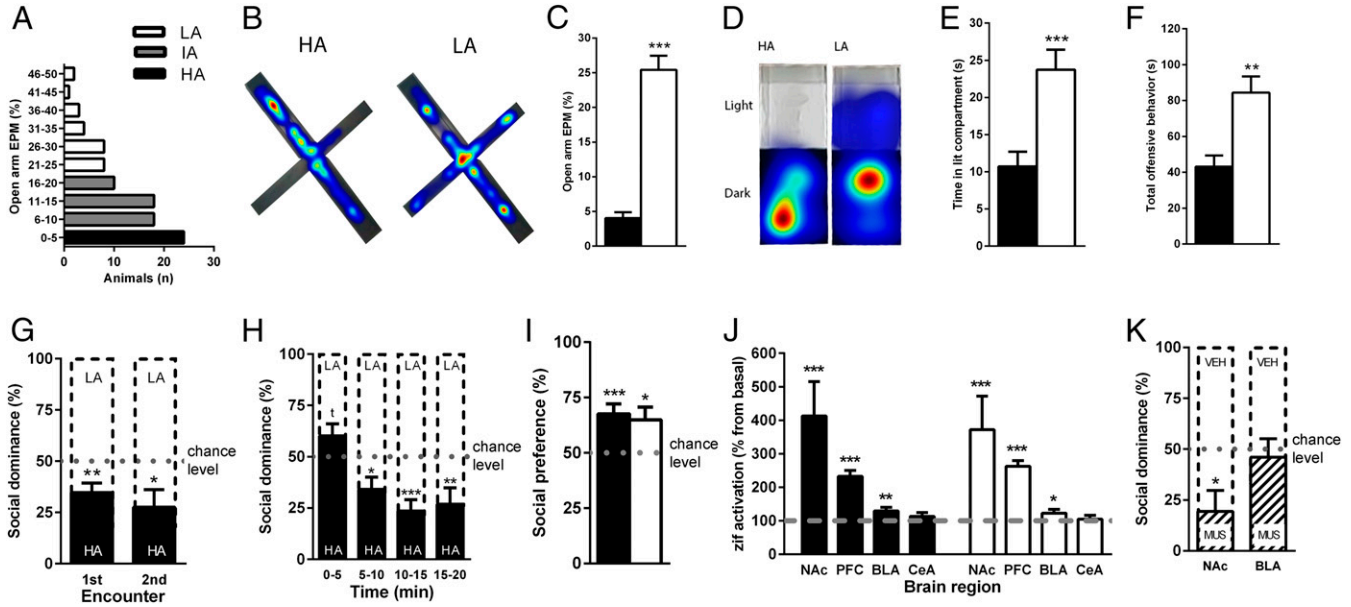

Fig. 1. High anxiety predisposes for social submission. (*A*) Classification for anxiety-profiles was based on the elevated plus maze (EPM; HA, high-anxious; IA, intermediate-anxious; LA, low-anxious). Time spent in the open arm of the EPM (*B* and *C*) and in the lit compartment of the light–dark test (*D* and *E*) was lower for HA animals, $n = 24$ per group. When competing against an LA rat, HA rats display reduced offensive behavior (*F*) and show low social dominance (*G*) emerging throughout time (*H*), $n = 24$ pairs. (*I*) Both HA and LA rats display similar levels of social preference. (*J*) Levels of *zif268* were increased following social competition in the nucleus accumbens (NAc), prefrontal cortex (PFC), and basolateral (BLA), but not central (CeA), amygdala in both groups, $n = 10$–20 per group. (*K*) Local inactivation with muscimol in the NAc, but not BLA, reduced social dominance, $n = 11$–13 pairs. Data are mean ± SEM (*$P < 0.05$, **$P < 0.01$, ***$P < 0.001$, Student's *t* test or one-sample *t* test against chance, 50%, level).

SI Appendix, Fig. S1 *E*–*G*), which is reflected by a social dominance level below chance (50%, Fig. 1*G*). Importantly, the subordinate character of high-anxious rats was not apparent from the onset of the interaction, but developed throughout the social encounter, indicating no lack of motivation to compete in these animals (Fig. 1*H*). The low competitive success of high-anxious rats was also evident during a subsequent encounter that took place 1 wk later (Fig. 1*G*), emphasizing the pervasive impact of anxiety on social rank. To examine whether this anxiety-related difference in social competitiveness was related to "social anxiety," we performed a follow-up study of social preference and found that both high- and low-anxious rats similarly exhibited a preference to explore a juvenile rat over an inanimate object (Fig. 1*I*). Thus, the differences in social competitiveness are not related to overall differences in social motivation or sociability. Because self-confidence is affected by stress (8), we investigated whether differences in the stress response might explain the low competitive success of high-anxious rats. We examined corticosterone levels in high- and low-anxious rats under basal conditions and following social competition. Although social competition did significantly increase corticosterone compared with baseline levels, there were no significant differences between anxiety groups at either time point (*SI Appendix*, Fig. S1*H*).

The Nucleus Accumbens Is Critically Involved in the Establishment of a Social Hierarchy. Several brain regions [e.g., the prefrontal cortex (15), NAc (16), and the amygdala (17, 18)] have been involved in the establishment of social hierarchies in rodents, with the ventral striatum (including the NAc) being consistently highlighted in human imaging studies of social status (19, 20) and competition (21). We confirmed the activation of the nucleus accumbens (along with that of the prefrontal cortex and basolateral, but not central, nucleus of the amygdala) following a social competition test, in both low- and high-anxious naïve animals by comparing the expression of the immediate early transcription factor gene *zif-268* mRNA following the encounter to basal conditions (Fig. 1*J*). We next aimed to test the causal involvement of the NAc and BLA in the establishment of a dominant rank. For this purpose, we performed independent experiments in which we pharmacologically inactivated each of these brain areas through microinfusion of muscimol, a $GABA_A$ receptor agonist, 30 min before social competition between two males matched for equivalent anxiety levels. Upon muscimol infusion in the NAc, rats exhibited reduced social dominance levels in a confrontation with another anxiety-matched male that was infused with vehicle (Fig. 1*K*). Importantly, this treatment did not induce changes in locomotor activity as evaluated in the open field (*SI Appendix*, Fig. S1*I*). On the contrary, inactivation of the basolateral amygdala (BLA) with muscimol had no impact on the social hierarchy outcome (Fig. 1*K*). We validated the effectiveness of our BLA treatment by demonstrating that it drastically inhibited fear conditioning (*SI Appendix*, Fig. S2), confirming the role of the BLA in this type of behavior (22). Given the prominent role of the NAc in social competition, we performed an additional experiment to gain insight into the cell types which show activation in this nucleus following a competitive encounter. Double-labeling of cFOS with markers for several neuronal types highlighted a significant activation of substance P-containing cells [known to represent medium spiny neurons (MSNs) containing the dopaminergic receptor D1 (23)] following social competition (Fig. 2 *A* and *B*) that correlated with the amount of competitive behavior (Fig. 2*C*). However, no social challenge-induced significant activations were observed for cholinergic cells, for cells containing enkephalin [known to represent D2-containing MSNs (23)] or for cells containing the S100 astrocytic marker (*SI Appendix*, Fig. S3 *A*–*F*). Therefore, these data point to the involvement of accumbal D1-containing MSNs in social competition.

High-Anxious Rats Exhibit Reduced Mitochondrial Function in the NAc. As our findings pointed to a prominent role of the NAc in social competition, we explored potential molecular pathways within the NAc differing between high- and low-anxious rats. We started by examining differential basal gene expression between high- and low-anxious rats in the NAc using microarrays and gene set

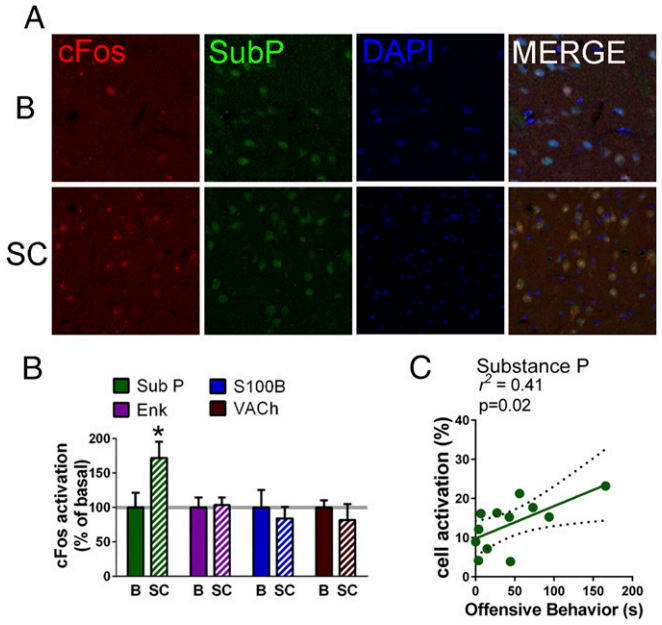

Fig. 2. D1-containing cells are activated by social competition. (*A* and *B*) cFOS activation of substance P (SubP; D1-containing cells), enkephalin (ENK; D2-containing cells), S100, and vesicular acetylcholine transporter (VAChT) in the NAc after social competition (SC) was compared with basal levels (B) and only substance P^+ cells displayed cFOS activation in response to social competition. (*C*) cFOS activation in substance P^+ cells significantly correlated with the duration of competitive offensive behavior. cFOS activation is presented as percentage of basal cFOS activation induced by social competition ($n = 6$ pairs per group) as mean ± SEM (*$P < 0.05$).

enrichment analysis (GSEA). The top regulated biological processes in high- versus low-anxious rats involved metabolic functions at various cellular levels (*SI Appendix*, Fig. S4*A*) and GSEA analysis on a curated set of mitochondrial genes pointed to significant differences in genes enriched in categories related to mitochondrial function (*SI Appendix*, Fig. S4*B* and Table S1). Mitochondrial respiratory function is essential for neural processing, as it plays key roles in many essential functions required for neural homeostasis and computations (24–26). Thus, we reasoned that the disadvantage of high-anxious rats to win the competition against low-anxious rats could reflect a lower mitochondrial activity in the NAc. We first measured protein levels in the five mitochondrial complexes that comprise the electron transport chain between high- and low-anxious rats. In both complexes I and II, starting points for mitochondrial respiration, high-anxious rats exhibited lower levels of protein than low-anxious rats (Fig. 3*A*). We then examined whether such protein differences might be indicative of a difference in mitochondrial number. However, both PCR analysis of mitochondrial DNA levels (Fig. 3*B*), and mitochondrial quantification from images obtained with transmission electron microscopy (*SI Appendix*, Table S2) revealed no significant differences in mitochondrial number or density in the NAc between high- and low-anxious rats, indicating that the observed differences in complex I and II protein content are not due to a sheer difference in mitochondrial number but to an enrichment in these respiratory complexes per mitochondria.

Accordingly, we next evaluated whether mitochondrial function in the NAc differed between high- and low-anxious rats. Using high-resolution respirometry, we found that when coupled respiration through complex I was stimulated in NAc homogenates by the addition of ADP, low-anxious rats displayed higher respiration rates than those of high-anxious rats, a difference that became more prominent upon complex II stimulation. Maximal electron transport system capacity (ETS) was also markedly higher in the NAc from low-anxious rats. Finally, the addition of rotenone revealed higher maximal respiration due to complex II activity (Fig. 3*C*). Linear regression analysis identified significant correlations between anxiety-like behavior on the elevated-plus maze and respiration levels following stimulation of complex II, ETS, and rotenone addition (*SI Appendix*, Fig. S5 *A–D*). The reduced mitochondrial respiratory capacity in the NAc of high-anxious animals is persistent in life, as it was also present when measured two months after anxiety characterization (Fig. 3*D*), fitting with the observed differences at the protein level (Fig. 3*A*). The addition of cytochrome *c* to the NAc preparations confirmed that the reported differences are not due to a differential mitochondrial vulnerability during experimental preparation (*SI Appendix*, Fig. S6*A*). Likewise, the anxiety-related effect on mitochondrial function was not a result of putative differences in body size, locomotor activity, or food intake, as these were equivalent for both high- and low-anxious animals (*SI Appendix*, Fig. S6 *B–D*). To investigate the specificity of these findings for the NAc, we examined mitochondrial respiration in the BLA. Here, unlike the NAc, high- and low-anxious rats displayed comparable respiration rates in the BLA (Fig. 3*E*).

We then examined whether the anxiety-related differences in NAc mitochondrial respiration had functional consequences for downstream mitochondrial outputs. First, we found that high-anxious animals exhibited significantly lower ATP concentrations in the NAc than low-anxious counterparts (Fig. 3*F*). Then, we measured the levels of a common ROS product in NAc homogenates, 4-Hydroxynonenal [(4-HNE; an α,β-unsaturated hydroxyalkenal produced by lipid peroxidation, with high levels suggesting increased periods of oxidative stress (27)] and found higher levels in high-anxious animals (Fig. 3*G*).

We then investigated the cellular specificity of the anxiety-related differences observed in NAc mitochondrial function. We performed mitochondrial respiration on synaptoneurosomal and glia-enriched fractions in three independent experiments (Fig. 3*H*) and found lower respiration in high-anxious compared with low-anxious animals in the synaptoneurosomal fraction only (Fig. 3 *I–J*). This finding is consistent with the lack of astrocytic activation induced by social competition (*SI Appendix*, Fig. S3*C*). Taken together, our results critically link anxiety with NAc mitochondrial function within the neuronal synaptic compartment (Fig. 3 *I–J*).

Manipulating Mitochondrial Function in the NAc Affects Social Dominance. Next, we inquired whether mitochondrial function in the NAc could per se be causally implicated in the outcome of a social hierarchy following a dyadic encounter. Given that both complex I- and complex II-dependent respiration were found to be associated with the anxiety phenotype (Fig. 3), we microinfused specific pharmacological inhibitors for each of these complexes [for complex I: rotenone (ROT); for complex II: the competitive inhibitor malonic acid (MA) and the noncompetitive 3-nitroproprionic acid (3NP)] into the NAc of separate groups of naïve animals that were paired to another anxiety-matched male infused with the corresponding vehicle. Microinfusion of either ROT, MA, or 3NP reduced the success of treated animals to win the social contest (Fig. 4*A*). Importantly, these treatments did not induce side effects on social investigation or auto-grooming during social competition (*SI Appendix*, Table S3), or alter locomotor activity (Fig. 4*B*), anxiety, or sociability (*SI Appendix*, Fig. S7 *A–D*) in additional experiments. Furthermore, these inhibitor treatments did not produce neurotoxic effects, as the drugs were infused at low doses and we confirmed the absence of lesion and neuronal death (*SI Appendix*, Fig. S8). The effects of complex I or complex II inhibition on social competition were specific for the NAc, as infusions of the same inhibitors into the BLA had no effect on social dominance and did not affect general locomotor activity (Fig. 4 *C* and *D*). We further showed

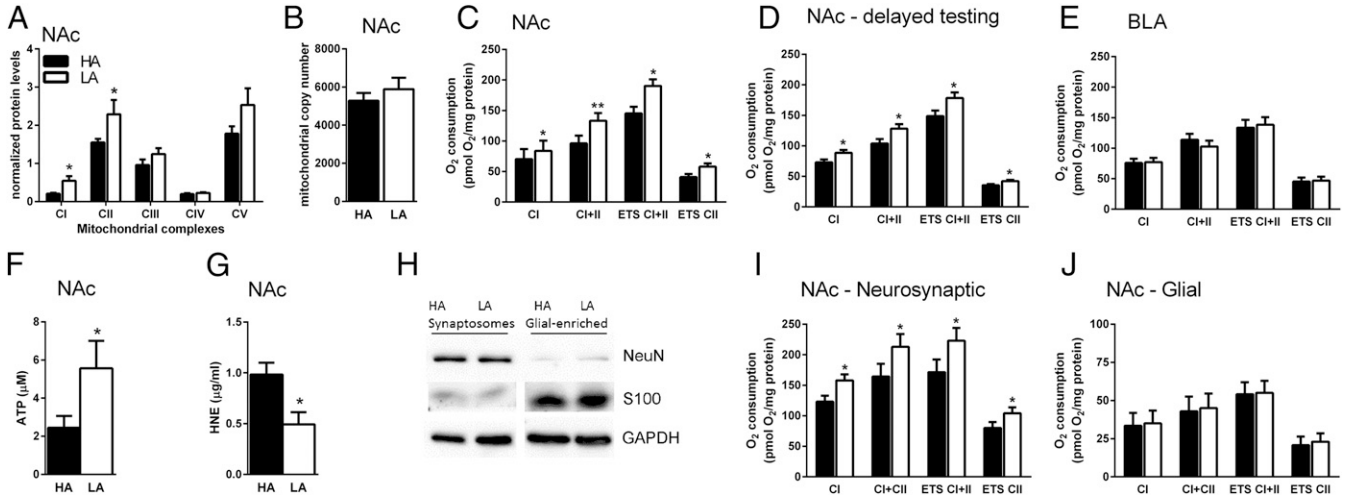

Fig. 3. High-anxious rats (HA) exhibit lower mitochondrial function that is specific to the nucleus accumbens (NAc). HA exhibit lower expression of complex I and II protein levels in the NAc than low-anxious rats (LA), $n = 5–12$ per group (*A*), but no significant difference in mitochondrial number, $n = 9$ per group (*B*). (*C*) HA display lower mitochondrial respiration in the NAc than LA, $n = 6$ per group. (*D*) These differences were also detected two months following anxiety characterization, $n = 8$ per group. (*E*) Mitochondrial respiration in the basolateral amygdala (BLA) does not differ between groups, $n = 11$ per group. ATP-levels in the NAc are lower in HA than LA, $n = 9–10$ per group (*F*), whereas ROS products are higher in HA, $n = 5–6$ per group (*G*). Synaptoneurosomes were separated from glia (*H*), and then mitochondrial respiration was measured in three independent experiments. The mitochondrial respiration deficit of HA is present in synaptoneurosomes (*I*) but not in glia-enriched fractions (*J*). Data are mean ± SEM. Respiration data are presented as estimated marginal means ± SEM of oxygen flux per mg tissue (*$P < 0.05$; **$P < 0.01$, Linear Mixed Model).

that, unlike infusion of muscimol in the BLA (*SI Appendix*, Fig. S2) that interferes with BLA-dependent auditory fear conditioning, microinfusion of 3NP did not affect conditioning in this task (*SI Appendix*, Fig. S2), discarding that neuronal inactivation could be a general mechanism whereby impairing mitochondrial function would affect putative functions from the affected brain region. Altogether, these data strongly support a key role for complex I- and II-dependent mitochondrial function within the NAc in the establishment of social dominance.

We then investigated whether we could reverse the disadvantage exhibited by high-anxious animals in the acquisition of social dominance by boosting NAc mitochondrial function. Nicotinamide adenine dinucleotide (NAD^+) is a metabolic cofactor present in cells that has been implicated in a wide range of critical metabolic activities (28). Treatment with the NAD^+ precursor nicotinamide (NAM; ref. 28), an amide form of vitamin B_3 that boosts mitochondrial respiration (29), into the NAc of high-anxious rats at a time point before the social encounter and at a dose that increased accumbal mitochondrial respiration (Fig. 5*A*), abolished the disadvantage of high-anxious animals to become dominant against low-anxious animals (Fig. 5*B*). Noteworthy, anxiety, sociability, social investigation and auto-grooming remained unaffected by NAM-treatment (*SI Appendix*, Fig. S7 *E* and *F* and Table S3). Finally, given the higher levels of the common ROS product 4HNE observed in high-anxious rats, we investigated whether treating these animals with the antioxidant Mitoquinone mesylate (mitoQ; ref. 30) in the NAc might enhance their dominance. Infusion of MitoQ at a time (3 h before testing) and dose (10 µM) that decreases accumbal 4HNE levels (Fig. 5*C*) had no effect on reversing the disadvantage of high-anxious rats when competing with vehicle-infused low-anxious rats (Fig. 5*D*). These observations suggest that the impact of mitochondrial function in social competition described here is not mediated by oxidative stress but is related to mitochondrial respiratory capacity. Taken together, our results point to a causal link between NAc mitochondrial function and social rank.

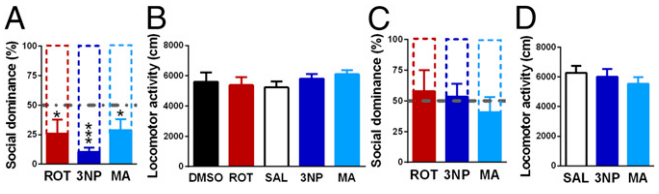

Fig. 4. Inhibition of mitochondrial complexes I and II in nucleus accumbens (NAc) decreased social dominance. Intra-NAc infusion of rotenone (ROT, $n = 12$ pairs), 3-nitropropionic acid (3-NP, $n = 10$ pairs), or malonic acid (MA, $n = 12$ pairs) reduced social dominance (*A*), without affecting locomotion in the Open Field, $n = 5–6$ per group (*B*). Intra-BLA infusions of ROT, 3-NP, or MA had no effect on social dominance, $n = 6$, 9, or 10 pairs, respectively (*C*), or locomotion, $n = 5$ per group (*D*). Data are mean ± SEM (**$P < 0.01$, ***$P < 0.001$, Student's *t* test or one-sample *t* test against chance level).

Discussion

In this study, we show that animals' anxiety trait is predictive of the outcome of a competitive social encounter and reveal critical neurobiological mechanisms underlying individual differences in the predisposition to win or lose a social competition. Our findings establish a key role for mitochondrial function in the NAc in the attainment of social dominance. Although mitochondrial involvement has been demonstrated in different mental health conditions, including anxiety disorders, stress and depression (10–12, 31, 32), our findings go beyond and establish a role for mitochondrial function in the regulation of individual differences in social behaviors under normal, nonpathological conditions.

First, following evidence in humans linking interindividual differences in anxiety with social status (7) and competitive self-confidence under stress (8), we showed that high-anxious rats tend to become subordinate when confronted with low-anxious rats. Importantly, the anxiety phenotype was reliably established through two validated tests for anxiety in rodents, and the pervasive impact of anxiety on social competition was confirmed through repeated social encounters (Fig. 1*G*). As the competing rats were matched for age, size, gender, and social experience, our findings suggested a role for intrinsic differences in neural mechanisms involved in social competition between high- and low-anxious individuals.

In our search for key brain regions involved in social hierarchy establishment, we obtained evidence for the involvement of the

NAc. First, we found a prominent activation of the NAc, particularly D1-containing cells, by social competition as highlighted through the assessment of the immediate early genes *zif*-268 and cFOS. Then, pharmacological inactivation of the NAc indicated the causal involvement of this brain region in social dominance. These findings are in line with previous evidence from lesion (33), neurochemical (34), and pharmacological (35) studies in rodents that highlight a causal involvement of the NAc in the development and/or expression of social dominance, as well as with data from human neuroimaging studies that show NAc activation under tasks involving social competition (21) or manipulation of social status (19, 20). Moreover, our findings are in agreement with current views that construe a critical role of the NAc in social operations, ranging from the processing of social information, to learning about conspecifics and making socially influenced decisions (36).

Additionally, the NAc has been classically implicated in different aspects of behavioral activation, including motivation, exertion of effort during instrumental behavior, reward-seeking and energy expenditure, as well as "vigor" of behavior (37–41). The NAc involvement seems to be particularly critical when there is ambiguity and/or uncertainty about which are the appropriate actions to be taken or under situations of instability and fluidity (42). Neural computations underlying these processes are all conceivably relevant for the evolving interactions entailed in the establishment of a social hierarchy. Importantly, a priori differences in motivation to win the social context cannot explain the outcome of the social competition between high- and low-anxious rats, as no differences in competitive behavior were observed during the early stages of the contest (Fig. 1*H*). Instead, the divergent ranks emerged progressively throughout the competition, indicating the potential for differential underlying metabolic capacity in the NAc.

Specifically, the key role for bioenergetics in the NAc in the differential predisposition of high- and low-anxious animals to win a social competition was identified by a number of converging data. Initial evidence in support of this concept was found in the microarray data indicating enrichment for metabolic and mitochondrial genes among those differentially expressed in the NAc between high- and low-anxious rats. Subsequently, data demonstrating lower complex I and II protein levels, mitochondrial respiration and ATP, but higher ROS products in the NAc of high anxious rats in comparison with low anxious counterparts further supported a link between variation in NAc bioenergetics and the attained social rank. The reduction in mitochondrial function was not simply a result of reduced mitochondrial number, as both high- and low-anxious rats exhibited similar mitochondrial number and densities in the NAc. Importantly, when we pharmacologically manipulated NAc mitochondrial respiration, we could directly influence social rank, which strongly supports the causal implication of differential anxiety-related NAc bioenergetics in the emergence of a dominance hierarchy. Inhibition of either complex I or complex II in the NAc markedly reduced social rank, whereas the competitive disadvantage of high-anxious animals to achieve a dominant rank against a low anxious male could be overcome by intra-NAc infusion of the mitochondrial booster vitamin B_3 (NAM). Control experiments excluded that the observed differences in social dominance between animals differing in anxiety and those impinged by the pharmacological treatments were not due to broad alterations in social behavior or confounded by perturbations in locomotion or general behavior. Nutritional interventions, such as vitamin B_3, have previously been proposed as therapeutics for depression and age-related neurodegenerative diseases (43, 44). Our results attribute a previously unidentified role for vitamin B_3 as a potential target to deal with anxiety-related deficits in competitiveness. However, pharmacological administration of the mitochondrial antioxidant MitoQ was ineffective to reverse the competitive disadvantage of high-anxious animals. Although these data are not supportive for a role of ROS in the subordinate outcome of high-anxious rats, we cannot discard the effectiveness of other antioxidant administration regimes (i.e., other administration timing, doses, and/or chronicity). Interestingly, although there is increasing evidence linking differences in mitochondrial function and oxidative stress with clinical pathologies such as anxiety disorders (31, 45–47), here we go beyond the pathological state and show that differences in brain mitochondrial function in the NAc can be found in association with personality differences.

In our study, several control experiments targeting the BLA suggested that the observed bioenergetic effects on social competition are specific to the NAc. Although these findings might seem surprising given the classical view of the BLA as a regulatory center for anxiety, anxiety modulation by the BLA has now been demonstrated to take place at its outputs, rather than within the BLA itself (reviewed in ref. 48). Given the proposed roles of the NAc in the regulation of behavioral vigor and exertion of effort, particularly in appetitively or aversely motivated behaviors (42), it is now tempting to speculate that the detected differences in mitochondrial function in the NAc as a function of anxiety could be critically involved in the decision-making processes weighing the amount of effort and/or cost exerted against the tradeoff of the prospect to win or, more generally, in defining differences in vulnerability to persist during sustained challenge.

The fact that suboptimal mitochondrial function in high-anxious rats was found in the NAc and not the BLA, suggests that the differences in the NAc could be secondary in this brain region and not a generalized mitochondrial dysfunction. Among the possible mechanisms involved, it is tempting to consider the participation of the dopaminergic system as several studies have linked high dopamine levels with reduced mitochondrial capacity in cells (49, 50). As we found activation of D1-containing cells following social competition, it is possible that differences in dopamine, as a function of anxiety, could contribute to the observed differences in mitochondrial function.

Substantial evidence implicates the NAc in depression (51, 52) and "anergia," or lack of energy at the core of depression and anxiety disorders (53, 54). Furthermore, mitochondrial deficiency is frequently observed in brain disorders (55), including depression (13, 14, 26, 31, 56) and anxiety (9). Moreover, individuals with mitochondrial disorders often express symptoms of depression and anxiety (10–13). High anxiety trait is a known vulnerability factor to develop depression, particularly if individuals are exposed to stress (57, 58), with stress impinging energetically costly neuronal adaptations (59, 60). Limited energy production due to reduced mitochondrial function may impair adaptive neuronal capacity to life

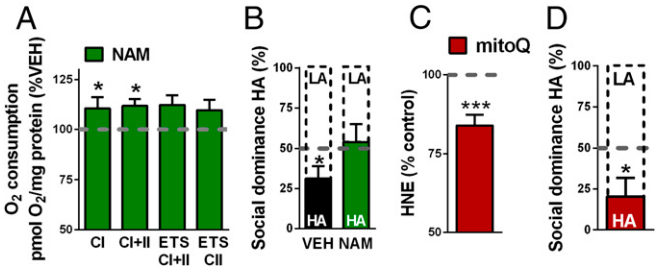

Fig. 5. Enhancing nucleus accumbens (NAc) energy stores via nicotinamide (NAM) infusion abolished the competitive disadvantage in high-anxious (HA) animals. (*A*) Intra-NAc infusion of NAM before social competition increased mitochondrial respiration in HA rats, $n = 7$ per group. (*B*) NAM-treated HA rats had similar chances to become dominant as low-anxious (LA) rats, $n =$ 9–11 pairs. Intra-NAc infusion of mitoquinone mesylate (mitoQ) reduced local ROS products (*C*), $n = 5$, but did not enhance social competition in HA rats (*D*), $n = 8$ pairs. Data are presented as mean ± SEM (*$P < 0.05$, ***$P < 0.001$, one sample *t* test against baseline or chance level).

challenges (32) and contribute to the development of psychopathologies (9, 10, 13, 14). Therefore, our results highlight differences in mitochondrial function in the NAc as a potential mechanism underlying the susceptibility or resilience to develop depression, and may open new prospects for the advancement of preventive therapeutic approaches to mood disorders.

Materials and Methods

Adult male Wistar rats (Charles River) weighing 250–275 g at the start of experiments were used. All experiments were performed with the approval of the Cantonal Veterinary Authorities (Vaud, Switzerland) and carried out in accordance with the European Communities Council Directive of 24 November 1986 (86/609EEC). Detailed descriptions of animal housing conditions, statistical analyses, and experimental methods are provided in the *SI Appendix, SI Materials and Methods*.

ACKNOWLEDGMENTS. We thank J. Grosse, I. Guillot de Suduiraut, K. Meng, E. Schranz, A. Thampi, S. Baliyan, E. T. Batzianouli, C. Maclachlan, and G. Knott for experimental assistance; and Drs. M. Kabbaj and M. Murphy for their generous gifts of the zif268 plasmid and mitoQ, respectively. This work was supported by grants from the Swiss National Science Foundation (31003A-152614; NCCR Synapsy) and intramural funding from the École Polytechnique Fédérale de Lausanne.

1. Sapolsky RM (2005) The influence of social hierarchy on primate health. *Science* 308(5722):648–652.
2. Neumann ID, Veenema AH, Beiderbeck DI (2010) Aggression and anxiety: Social context and neurobiological links. *Front Behav Neurosci* 4:12.
3. Fuxjager MJ, et al. (2010) Winning territorial disputes selectively enhances androgen sensitivity in neural pathways related to motivation and social aggression. *Proc Natl Acad Sci USA* 107(27):12393–12398.
4. Oliveira RF, Silva A, Canario AV (2009) Why do winners keep winning? Androgen mediation of winner but not loser effects in cichlid fish. *Proc Biol Sci* 276(1665):2249–2256.
5. Boyce WT (2004) Social stratification, health, and violence in the very young. *Ann N Y Acad Sci* 1036:47–68.
6. Allan S, Gilbert P (1997) Submissive behaviour and psychopathology. *Br J Clin Psychol* 36(Pt 4):467–488.
7. Gilbert P, McEwan K, Bellew R, Mills A, Gale C (2009) The dark side of competition: How competitive behaviour and striving to avoid inferiority are linked to depression, anxiety, stress and self-harm. *Psychol Psychother* 82(Pt 2):123–136.
8. Goette L, Bendahan S, Thoresen J, Hollis F, Sandi C (2015) Stress pulls us apart: Anxiety leads to differences in competitive confidence under stress. *Psychoneuroendocrinology* 54:115–123.
9. Tyrka AR, et al. (2015) Alterations of mitochondrial DNA copy number and telomere length with early adversity and psychopathology. *Biol Psychiatry*, 10.1016/j.biopsych.2014.12.025.
10. Streck EL, et al. (2014) Mitochondria and the central nervous system: Searching for a pathophysiological basis of psychiatric disorders. *Rev Bras Psiquiatr* 36(2):156–167.
11. Morava E, Kozicz T (2013) Mitochondria and the economy of stress (mal)adaptation. *Neurosci Biobehav Rev* 37(4):668–680.
12. Anglin RE, Mazurek MF, Tarnopolsky MA, Rosebush PI (2012) The mitochondrial genome and psychiatric illness. *Am J Med Genet B Neuropsychiatr Genet* 159B(7):749–759.
13. Morava E, et al. (2010) Depressive behaviour in children diagnosed with a mitochondrial disorder. *Mitochondrion* 10(5):528–533.
14. Koene S, et al. (2009) Major depression in adolescent children consecutively diagnosed with mitochondrial disorder. *J Affect Disord* 114(1-3):327–332.
15. Wang F, et al. (2011) Bidirectional control of social hierarchy by synaptic efficacy in medial prefrontal cortex. *Science* 334(6056):693–697.
16. Beiderbeck DI, et al. (2012) High and abnormal forms of aggression in rats with extremes in trait anxiety–involvement of the dopamine system in the nucleus accumbens. *Psychoneuroendocrinology* 37(12):1969–1980.
17. Kumaran D, Melo HL, Duzel E (2012) The emergence and representation of knowledge about social and nonsocial hierarchies. *Neuron* 76(3):653–666.
18. Machado CJ, Bachevalier J (2006) The impact of selective amygdala, orbital frontal cortex, or hippocampal formation lesions on established social relationships in rhesus monkeys (Macaca mulatta). *Behav Neurosci* 120(4):761–786.
19. Zink CF, et al. (2008) Know your place: Neural processing of social hierarchy in humans. *Neuron* 58(2):273–283.
20. Ly M, Haynes MR, Barter JW, Weinberger DR, Zink CF (2011) Subjective socioeconomic status predicts human ventral striatal responses to social status information. *Curr Biol* 21(9):794–797.
21. Le Bouc R, Pessiglione M (2013) Imaging social motivation: Distinct brain mechanisms drive effort production during collaboration versus competition. *J Neurosci* 33(40): 15894–15902.
22. Wilensky AE, Schafe GE, LeDoux JE (1999) Functional inactivation of the amygdala before but not after auditory fear conditioning prevents memory formation. *J Neurosci* 19(24):RC48.
23. Le Moine C, Bloch B (1995) D1 and D2 dopamine receptor gene expression in the rat striatum: Sensitive cRNA probes demonstrate prominent segregation of D1 and D2 mRNAs in distinct neuronal populations of the dorsal and ventral striatum. *J Comp Neurol* 355(3):418–426.
24. Nicholls DG, Budd SL (2000) Mitochondria and neuronal survival. *Physiol Rev* 80(1):315–360.
25. Cheng A, Hou Y, Mattson MP (2010) Mitochondria and neuroplasticity. *ASN Neuro* 2(5):e00045.
26. Manji H, et al. (2012) Impaired mitochondrial function in psychiatric disorders. *Nat Rev Neurosci* 13(5):293–307.
27. Esterbauer H, Schaur RJ, Zollner H (1991) Chemistry and biochemistry of 4-hydroxynonenal, malonaldehyde and related aldehydes. *Free Radic Biol Med* 11(1):81–128.
28. Houtkooper RH, Cantó C, Wanders RJ, Auwerx J (2010) The secret life of NAD+: An old metabolite controlling new metabolic signaling pathways. *Endocr Rev* 31(2): 194–223.
29. Nowak R, et al. (2010) Effect of selected NAD+ analogues on mitochondria activity and proliferation of endothelial EA.hy926 cells. *Eur J Pharmacol* 640(1-3):102–111.
30. Murphy MP, Smith RA (2007) Targeting antioxidants to mitochondria by conjugation to lipophilic cations. *Annu Rev Pharmacol Toxicol* 47:629–656.
31. Gardner A, Boles RG (2011) Beyond the serotonin hypothesis: Mitochondria, inflammation and neurodegeneration in major depression and affective spectrum disorders. *Prog Neuropsychopharmacol Biol Psychiatry* 35(3):730–743.
32. Picard M, Juster RP, McEwen BS (2014) Mitochondrial allostatic load puts the 'gluc' back in glucocorticoids. *Nat Rev Endocrinol* 10(5):303–310.
33. Fantin G, Bottecchia D (1984) Effect of nucleus accumbens destruction in rat. *Experientia* 40(6):573–575.
34. Anstrom KK, Miczek KA, Budygin EA (2009) Increased phasic dopamine signaling in the mesolimbic pathway during social defeat in rats. *Neuroscience* 161(1):3–12.
35. Puciłowski O, Trzaskowska E, Kostowski W, Wośko W (1988) Inhibition of affective aggression and dominance in rats after thyrotropin-releasing hormone (TRH) microinjection into the nucleus accumbens. *Peptides* 9(3):539–543.
36. Bhanji JP, Delgado MR (2014) The social brain and reward: Social information processing in the human striatum. *Wiley Interdiscip Rev Cogn Sci* 5(1):61–73.
37. Robbins TW, Everitt BJ (2007) A role for mesencephalic dopamine in activation: Commentary on Berridge (2006). *Psychopharmacology (Berl)* 191(3):433–437.
38. Beeler JA, Frazier CR, Zhuang X (2012) Putting desire on a budget: Dopamine and energy expenditure, reconciling reward and resources. *Front Integr Nuerosci* 6:49.
39. Niv Y, Daw ND, Joel D, Dayan P (2007) Tonic dopamine: Opportunity costs and the control of response vigor. *Psychopharmacology (Berl)* 191(3):507–520.
40. Salamone JD, Correa M, Nunes EJ, Randall PA, Pardo M (2012) The behavioral pharmacology of effort-related choice behavior: Dopamine, adenosine and beyond. *J Exp Anal Behav* 97(1):125–146.
41. Treadway MT, Bossaller NA, Shelton RC, Zald DH (2012) Effort-based decision-making in major depressive disorder: A translational model of motivational anhedonia. *J Abnorm Psychol* 121(3):553–558.
42. Floresco SB (2015) The nucleus accumbens: An interface between cognition, emotion, and action. *Annu Rev Psychol* 66:25–52.
43. Bodnar LM, Wisner KL (2005) Nutrition and depression: Implications for improving mental health among childbearing-aged women. *Biol Psychiatry* 58(9):679–685.
44. Liu D, et al. (2013) Nicotinamide forestalls pathology and cognitive decline in Alzheimer mice: Evidence for improved neuronal bioenergetics and autophagy procession. *Neurobiol Aging* 34(6):1564–1580.
45. Einat H, Yuan P, Manji HK (2005) Increased anxiety-like behaviors and mitochondrial dysfunction in mice with targeted mutation of the Bcl-2 gene: Further support for the involvement of mitochondrial function in anxiety disorders. *Behav Brain Res* 165(2):172–180.
46. Hovatta I, et al. (2005) Glyoxalase 1 and glutathione reductase 1 regulate anxiety in mice. *Nature* 438(7068):662–666.
47. Rammal H, Bouayed J, Younos C, Soulimani R (2008) Evidence that oxidative stress is linked to anxiety-related behaviour in mice. *Brain Behav Immun* 22(8):1156–1159.
48. Lalumiere RT (2014) Optogenetic dissection of amygdala functioning. *Front Behav Neurosci* 8:107.
49. Rosenfeld M, Brenner-Lavie H, Ari SG, Kavushansky A, Ben-Shachar D (2011) Perturbation in mitochondrial network dynamics and in complex I dependent cellular respiration in schizophrenia. *Biol Psychiatry* 69(10):980–988.
50. Brenner-Lavie H, et al. (2008) Dopamine modulates mitochondrial function in viable SH-SY5Y cells possibly via its interaction with complex I: Relevance to dopamine pathology in schizophrenia. *Biochim Biophys Acta* 1777(2):173–185.
51. Nestler EJ, Carlezon WA, Jr (2006) The mesolimbic dopamine reward circuit in depression. *Biol Psychiatry* 59(12):1151–1159.
52. Chaudhury D, et al. (2013) Rapid regulation of depression-related behaviours by control of midbrain dopamine neurons. *Nature* 493(7433):532–536.
53. Stahl SM (2002) The psychopharmacology of energy and fatigue. *J Clin Psychiatry* 63(1):7–8.
54. Demyttenaere K, De Fruyt J, Stahl SM (2005) The many faces of fatigue in major depressive disorder. *Int J Neuropsychopharmacol* 8(1):93–105.
55. Lin MT, Beal MF (2006) Mitochondrial dysfunction and oxidative stress in neurodegenerative diseases. *Nature* 443(7113):787–795.
56. Chang CC, Jou SH, Lin TT, Liu CS (2014) Mitochondrial DNA variation and increased oxidative damage in euthymic patients with bipolar disorder. *Psychiatry Clin Neurosci* 68(7):551–557.
57. Sandi C, Richter-Levin G (2009) From high anxiety trait to depression: A neurocognitive hypothesis. *Trends Neurosci* 32(6):312–320.
58. Castro JE, et al. (2012) Personality traits in rats predict vulnerability and resilience to developing stress-induced depression-like behaviors, HPA axis hyper-reactivity and brain changes in pERK1/2 activity. *Psychoneuroendocrinology* 37(8):1209–1223.
59. de Kloet ER, Joëls M, Holsboer F (2005) Stress and the brain: From adaptation to disease. *Nat Rev Neurosci* 6(6):463–475.
60. McEwen BS (2012) Brain on stress: How the social environment gets under the skin. *Proc Natl Acad Sci USA* 109(Suppl 2):17180–17185.

Supplementary Materials:

Materials and Methods

Figures S1-S8

Table S1-3

References (1-13)

Materials and Methods:

Animals. Adult male wistar rats were used for all experiments. Animals were individually housed in polypropylene cages (57 x 35 x 20 cm) with abundant pine bedding in a temperature- (23C) and light- (0700-1900 h) controlled room. All animals had *ad libitum* access to standard food and water. Upon arrival to the facility, animals were allowed to habituate to the vivarium for one week and were then handled for 2 min/d during 3 days prior to the start of all experiments. All behavioral manipulations were performed during the light phase by experimenters blind to treatment groups. Unless otherwise indicated, all animals were first characterized for trait anxiety and then sacrificed under basal conditions for ex-vivo analyses. All efforts were made to minimize the number of animals while maintaining statistical rigor.

Statistical analyses. All samples represent biological replicates. Sample sizes are indicated in the figure legends. Unpaired two-tailed Student's t-tests were used to compare sets of data obtained from independent groups of animals. In follow-up experiments, unpaired one-tailed Student's t-tests were used to confirm previous findings. Within-pair amounts of behavior in the social competition test were compared using paired two-tailed Student's t-tests. In sets of data in which animals were matched for anxiety, relative social dominance scores were compared using one-sample t-tests against chance (50%). When necessary, data were transformed to obtain symmetric distributions for statistical analysis. Figures are presented with original, non-transformed data. All data –except for mitochondrial respiration- were analyzed using Prism version 5.01 (Graphpad software Inc., San Diego, CA). For respiration experiments, data were analyzed using SPSS statistical software version 13.0 (SPSS, Chicago, IL). As experiments were performed in blocks across days, a linear mixed model was created that included block as a random effect in addition to fixed effects of either anxiety or treatment (where appropriate). The estimated marginal means of the model are then reported. P-values are reported in figure legends, with the second decimal rounded to the nearest figure. Statistical significance was considered at the $p<0.05$ level.

Elevated Plus Maze. Prior to the testing for social hierarchy, animals were tested for anxiety-related behavior in the EPM as previously described (1). Lighting was maintained at 15-16 lx on the open arms and 5-7 lx in the closed. Depending on the amount of time spent on the open arm animals were classified as high- (HA, ≤5% open arm duration) intermediate (IA, 6-20 % open arm duration) or low-anxious (LA, ≥20% open arm duration). Before and in between testing the apparatus was cleaned with a 5 % EtOH solution.

Light-Dark box. To ascertain that the anxiety-like behavior measured in the EPM is indeed a reliable indicator for anxiety; animals were also tested in the light-dark box, 2 d after EPM-exposure. The apparatus and procedure are the same as that described in a previous publication (1), with the modification of lighting intensity. One chamber was black (dark box) and kept at 20lx while the other chamber was white (light box) with an illumination level of 160lx. Before and in between testing the apparatus was cleaned with a 5% EtOH solution.

Social hierarchy test. Rats were pair-wise matched for weight but, depending on the purpose of the experiment, animals in each pair were either of a similar or opposite anxiety profile. In experiments that aimed at disentangling the impact of anxiety in the formation of a social hierarchy, rat pairs were composed of a high- and a low-anxious rat. In pharmacological experiments addressed to investigate the impact of specific treatments on social dominance, pairs of animals were matched for similar anxiety levels; i.e., the rats in each dyad were considered equal in their probability (= 50%) to become dominant or subordinate during their encounter.

As previously described (2), animals were marked on their body for identification and placed in pairs in a clean (neutral) cage without food or water for 20 min. During the social hierarchy test both rats displayed spontaneously offensive behavior, but this balance typically shifted in the favor of one animal towards the end of the test. Social dominance was estimated by summation of the total duration of offensive behaviors for each rat in the dyad (offensive upright, lateral threat and keeping-down behavior, as previously described (3)). Earlier we found that social dominance in these encounters correlate with the outcome in competition for water or for food rewards (1). During pilot studies, we found that infrequently offensive behavior was virtually absent during social encounter (no rat displaying >10s of total offensive behavior); these pairs were excluded from analysis as the relative social dominance in these pairs cannot be reliably measured. Auto-grooming and social investigation was taken into account to determine the specificity of the drug-effects on offensive behavior.

Social preference test. The social preference test was performed in a rectangular, three-chambered box that included a central compartment where the rat was initially placed. Thereafter, retractable doors were removed and the rat could explore the left- and right-compartment for 5 min. The left- and right-compartments were equipped with a floor-fixed transparent perforated Plexiglas cylinder that contained either an unfamiliar male juvenile rat or an unfamiliar object. The time spent sniffing either the juvenile (social target) or the novel object (inanimate target) was manually scored from videotapes by an experimenter who was blinded to the treatment groups.

Open Field test. The open field was used to determine the effects of intra-NAc and intra-BLA infusion of the mitochondrial complex I-and II inhibitors rotenone, 3-nitroproprionic acid, and malonic acid on locomotor behavior. The open field apparatus and procedure were previously described (1). The light was adjusted to a level of 8-10 lx in the center of the arena.

In situ hybridization. Rats were characterized for anxiety and sacrificed either under basal conditions or 5 min after a paired social competitive encounter. Brains were rapidly dissected out, frozen at -30°C in isopentane and stored at -80°C until further processing. 20μm sections were obtained on a freezing cryostat and prepared and hybridized as previously described (4). An outline was created for each region of interest from the left and right sides of the brain from rostral/caudal sections. The radioactive signal was quantified from 8-12 brain sections per region per rat using MCID Image Analysis software (MCID, UK). Optical density values were background-corrected, multiplied by the area sampled to produce an integrated density measurement, and then averaged to produce one data point for each brain region for each animal for statistical analysis.

Corticosterone Analysis. Rats were characterized for anxiety and sacrificed either in basal conditions or 5 min after a paired social competitive encounter. Trunk blood was collected and centrifuged at 12,000 rpm to isolate plasma. 10μL of plasma sample were then prepared according to manufacturer's instructions to measure corticosterone concentrations using a corticosterone ELISA kit (Enzo Life Sciences, ADI-901-097). Levels were calculated using a standard curve method.

Intracerebral cannulation surgery. Rats subjected to pharmacological experiments were implanted bilateral with stainless steel guide cannulas aimed at the NAc or BLA. Rats were anesthetized by isoflurane inhalation (induction 4% isoflurane for 4 min and maintenance 2.5% isoflurane in O_2 at a flow of 4L/min) and placed in a stereotaxic apparatus (David Kopf Instruments, Tujunga, CA, USA). Small holes were drilled through the skull for bilateral placement of stainless steel 22 gauge guide cannulae (Plastics One, Roanoke, VA, USA) fitted with a removable dummy cannula. Coordinates were based on the atlas of Paxinos and Watson (5) and are taken from bregma (in mm) for NAc: A.P. +1.2, M.L. ±1.5, D.V. -6.50 and for BLA: A.P. -2.80, ± 4.90, D.V. -7.50. Cannulae were fixed to the skull with two anchoring screws and dental acrylic (Duralay 2244; Reliance, Worth, IL). After behavioral experiments animals were sacrificed by i.p. pentobarbital injection and correct cannulae placements was routinely verified with Evans blue histology.

Drug infusions. Behavioral experiments involving mitochondrial complex inhibitors were performed 10 min after drug administration. Behavioral experiments involving pharmacological inactivation were performed 30 min after drug administration. We randomly assigned animals to their respective treatment. For intra-cerebral infusions the dummy was removed and an injector was inserted that extended 1- (BLA) or 2mm (NAc) from the tip of the cannulae. All drugs were bilaterally infused in a total volume of 0.3 μL during 1 min of constant flow. The injector remained in place for one additional minute after infusion to allow proper diffusion. 0.224nM rotenone (complex I-inhibitor, Sigma-Aldrich) was dissolved in DMSO. 0.849nM Malonic Acid and 0.742nM 3-nitroproprionic acid (complex II-inhibitors, Sigma-Aldrich) were dissolved in saline. Muscimol (Tocris Biosciences, Bristol, UK) was dissolved in saline. All inhibitors were infused at a dose of 25ng. Mitoquinone mesylate (mitoQ) was dissolved in saline with 10% DMSO and bilaterally infused (0.5 μL) at a concentration of 10μM

3 h prior to social competition or brain sampling for the assessment of 4HNE. 57.8 nM nicotinamide (NAM, Sigma-Aldrich) was dissolved in saline and bilaterally infused at a dose of 2μg 3 h prior to social competition or respirometry. No animal received a repeated ETC drug infusion.

Auditory Fear Conditioning. Naïve rats received intra-BLA infusions of saline, 3-nitroproprionic acid, or muscimol prior to the training session of auditory fear conditioning. Animals were tested for acquisition of the fear memory by exposure to the auditory stimulus one week after training. Training and testing took place in a rodent fear conditioning cage (30×37×25 cm) placed into a sound-attenuating chamber. The side walls of the fear conditioning cage were constructed of white metacrylate, while the door and the top cover were Plexiglas. The floor consisted of 20 steel rods through which a scrambled shock from a shock generator could be delivered (Panlab, S.L., Barcelona, Spain). Following drug infusions, the animals were placed in the conditioning chambers. During the training session, rats were exposed to one context (consisting of white rectangular walls, a steel grid floor, white lights, that was cleaned with 5% ethanol before each trial) for a duration of 160s, followed by three presentations of tone-shock pairings in which the tone (20s, 80dB, 800Hz) co-terminated with a foot shock (0.6mA, 1s). The intertone interval was 40s. One week after the training session, the animals underwent a test session in a novel context (metallic grid walls, a gray plastic floor, green lights, that was cleaned with 1% acetic acid before each trial) for 8 min where the same training tone was presented during the last 5 min. Acquisition of fear was quantified as the amount of time the rats spent freezing during the testing session. Freezing was defined as the lack of all movement (except for respiratory-related movements).

Triple labeling Immunofluorescence. *Preparation.* Rats were anaesthetized with a lethal dose of pentobarbital and sacrificed by transcardial perfusion using 0.9% saline solution followed by a fixative solution of paraformaldehyde 4% in PBS (pH=7.5). The brains were removed, post-fixed for 4 h in 4% paraformaldehyde/PBS and cryoprotected in 30% sucrose/PBS. Coronal sections (30 µm thick) were cut on a cryostat (Leica, CM3050 S), and free-floating sections were triple labeled for cFOS, DAPI, and one of four antibodies against the main cell-types of the NAc. The floating sections were rinsed briefly with PBS then blocked 1 h in PBS - 0.1% Triton X-100 (Sigma-Aldrich) - 5% normal donkey serum (Jackson ImmunoResearch) and incubated overnight at 4 °C with rabbit anti-cFOS (Milllipore, ABE457, 1:500) and one of the following: goat anti-Substance P (for staining of D1-containing cells, Santa Cruz, sc-9758, 1:100), mouse anti-S-100 (for staining of astrocytes, Abcam, ab4066, 1:100), or goat anti-vesicular acetylcholine transporter (VAChT, for staining of cholinergic cells, Millipore, ABN100, 1:2,000). Rabbit anti-Met Enkephalin (for staining of D2-containing cells, Abcam, ab22620, 1:1,000) was incubated with goat anti-cFOS (Santa Cruz, sc-52-G, 1:50). Both cFOS antibodies were confirmed as exhibiting similar staining in a cFOS/cFOS double labeled control experiment. The sections were washed in PBS and incubated for 2 h at room temperature with the secondary antibodies: donkey-anti-rabbit IgG Alexa 568 conjugate (Lifetechnologies, A10042, 1:1,000), donkey anti-goat IgG Alexa 488 conjugate (Lifetechnologies, A11055, 1:800) or goat anti-mouse IgG Alexa Fluor 488 conjugate (Lifetechnologies, A11029, 1:800). After washing in PBS the sections were incubated 10 minutes in DAPI (Sigma,

1:10,000), rinsed and mounted with Fluoromount-G (SouthernBiotech). Images were captured with a confocal microscope (Zeiss, LSM700) using a × 20 objective. The sample images were captured at the same coordinates for each animal. A mosaic of 16 images were captured and stitched together for one hemisphere. For visualization purposes, representative regions within specific sections were zoomed and enhanced in a linear manner for brightness and contrast using FIJI software. Enhanced images were then arranged within photoshop CS (Adobe). Quantification was performed on original, unenhanced images only.

Quantification of immunofluorescence LSM images were stitched together using the grid stitching plug-in for FIJI (6). The backgrounds of each channel were measured at five different random areas around the section and averaged together to generate a mean background for each channel. This mean background was then subtracted from each channel. Cells were delineated using a Huang threshold to label only those stained with DAPI within 20-200 pixels. The number of these cells that were also labeled with cFOS and the antibody of interest were counted and converted to a percentage of the total number of DAPI-stained cells for each section. Sections were then averaged to provide one value per animal per cell-type of interest.

Microarray. Naïve rats were characterized for trait anxiety on the elevated plus maze (high-, intermediate-, and low- anxious rats, n=5/group) and were sacrificed under basal conditions by rapid decapitation. Brains were flash frozen and NAc were tissue-punched on a freezing cryostat with a 2.0mm tissue punch (Harris UniCore, USA). RNA was extracted using Ambion RNaqueous-micro kit (Life Technologies) which were then converted to cDNA libraries using Nugen Ovation Pico WTA system v2 reaction kits (Nugen, USA). cDNA was fragmented and labeled using the Encore Biotin Module (Nugen, USA) and hybridized to Affymetrix 1.0 Exon ST arrays (Affymetrix). The arrays were scanned to produce raw signal intensity values for all probes. These values were then preprocessed using the Robust Multichip Average algorithm (RMA; (7). Gene expression was analyzed using the *limma* package (8) within Bioconductor (9) in order to generate a model that treated anxiety as a linear predictor and produce a rank-ordered list of p-values. This rank-ordered list was then used to perform gene enrichment analysis using the GSEA software (10). We first searched for significantly associated gene sets within the C5 subclass (GO gene sets), taking a cutoff of a nominal p-value of 0.10. As the top biological processes that were differentially regulated between anxiety phenotypes were metabolic, we then examined our data for enrichment of mitochondrial genes using a custom curated gene set.

Western Blots. Rats were sacrificed under basal conditions by rapid decapitation and the nucleus accumbens was tissue-punched on a freezing cryostat with a 2.0 mm tissue punch (Harris UniCore). Briefly, tissue was homogenized in ten volumes of ice-cold sucrose (0.32 M) and HEPES (5 mM) buffer that contained a cocktail of protease inhibitors (Complete TM, Roche, UK) with 16 strokes and centrifuged at 1, 000 x g for 5 min. The resulting total fraction pellet was resuspended in Krebs buffer with 1% NP-40, incubated at 4°C for 40 min, and then centrifuged at 10,000 x g for 20 min at 4°C. Protein concentration for each sample was estimated by BCA protein analysis (Bio-Rad). 15μg of protein were loaded in each well and then separated on 10% (w／v) SDS-PAGE and transferred (70V, 1.5 h) to a nitrocellulose membrane (Whatman). Multiple gels were loaded in a counterbalanced manner and run simultaneously for

two separate experiments. After saturation of the nonspecific sites with 5% (w/v) skim milk in PBST, the blots were incubated overnight at 4C with primary antibodies against the mitochondrial complexes I-V (MitoProfile Total OXPHOS Rodent WB Antibody cocktail, MitoSciences, cat No. MS604). Polyclonal mouse anti-rat antibodies for Actin (1:30,000; Life Technologies, cat. No.9485) were incubated as loading controls. The blots were washed with PBST, incubated for 1 h with a secondary antibody, an anti-rabbit (anti-mouse for loading controls) Ig peroxidase conjugate (whole molecule conjugate; diluted 1:10,000; Sigma) and finally developed using an enhanced chemiluminescence (ECL) system (Pierce). For the quantification, bands were revealed with a ChemiDoc imaging system (Bio-Rad) for optimum exposure time. Images were then analysed using QuantityOne software v4.6.3 (Bio-Rad) where the adjusted volume was calculated and recorded for each band. For each group, adjusted values were normalized to Actin.

Mitochondrial Copy Number. Rats were sacrificed under basal conditions by rapid decapitation and the nucleus accumbens was rapidly dissected out, frozen at -30°C in isopentane, and stored at -80°C until further processing. Tissue was placed in lysis buffer and DNA was extracted using DNeasy extraction kit (Qiagen). DNA concentrations were measured using the Nanodrop. Oligonucleotide primers for real-time quantitative PCR and tested to ensure all efficiencies were above 95%. All primers were efficient between 97.8 and 99.7%. Primers tested includ: ND1, fwd TCCTCTTATCCGTCCTCCTAATAA; rev CAGGCGGGGATTAATAGTCA; GAPDH, fwd AAACCCATCACCATCTTCCA; rv CCTCGAAGTACCCTGTGCAT. Each reaction contained 200 nM each of the forward and reverse primers, SYBR Green PCR Master Mix (Applied Biosystems) and 10 ng sample DNA in a 20 µl reaction volume. The qPCR reactions were performed in triplicates in an ABI Prism 7900 Sequence Detection System (Applied Biosystems). The standard cycling conditions were 95°C for 5 min, followed by 40 cycles of 95°C for 30 s, and 60°C for 30 s. Melt curves were generated at the end of the regular qPCR cycles.The comparative Ct method was used to determine raw copy number. MtDNA levels were normalized to the nuclear-encoded gene, GAPDH.

Electron Microscopy. *Preparation.* Rats were anaesthetized with a lethal dose of pentobarbital and then sacrificed under basal conditions by transcardial perfusion of 2.5% glutaraldehyde and 2% paraformaldehyde in 0.1M PB (pH7.4). The brains removed 2h after perfusion. Sections (80 µm) were cut in the coronal plane at the level of the NAc. Sections where washed in cacodylate buffer (0.1M, pH 7.4) and postfixed in 1% osmium tetroxide/1.5% potassium ferrocyanide, 1% osmium tetroxide, and 1% uranyl acetate, each fixation step lasting 40 min. The sections were dehydrated in increasing ethanol concentrations, before being washed in propylene oxide, and infiltrated with Epon resin. Sections where then flat embedded between two glass slides coated in mold releasing agent (Hobby time, Glorex, Switzerland) and polymerized at 60°C for 24h. Sections (50nm) where then cut through the NAc using a diamond knife and collected onto copper slot grids with a pioloform support film.

Imaging. Sections were imaged with a transmission electron microscope (Tecnai Spirit, FEI company, Eindhoven, The Netherlands) at 80 KeV and a magnification of 2.29nm x 2.29nm per pixel and images captured with a CCD camera (4k x 4k Eagle camera, FEI company).

Quantification. Mitochondrial density and size were measured blind using the TrakEM2 software in Fiji (11). A counting square, with an area of 66.9 μm^2, was drawn on each image. Mitochondria inside this square, as well as those touching the top and right edges (inclusion lines), were counted. Those touching the bottom and left were excluded (exclusion lines). The largest diameter was measured, and mitochondria were also classified as to whether they were seen in dendrites, or elsewhere. A total of 377 counting squares were analyzed from 6 animals (n = 3/group for high- and low-anxious rats).

Mitochondria Respirometry. Animals were characterized for anxiety and sacrificed under basal conditions by rapid decapitation and the nucleus accumbens and basolateral amygdala were rapidly dissected out, weighed, and placed in a petri dish on ice with 2 mL of relaxing solution (2.8 mM Ca_2K_2EGTA, 7.2 mM K_2EGTA, 5.8 mM ATP, 6.6 mM $MgCl_2$, 20 mM taurine, 15 mM sodium phosphocreatine, 20 mM imidazole, 0.5 mM dithiothreitol and 50 mM MES, pH = 7.1) until further processing. Tissue samples were then gently homogenized in ice-cold respirometry medium (MiR05: 0.5 mM EGTA, 3mM $MgCl_2$, 60 mM potassium lactobionate, 20 mM taurine, 10 mM KH_2PO_4, 20 mM HEPES, 110 mM sucrose and 0.1% (w/v) BSA, pH=7.1) with an eppendorf pestle. Then, 2 mg of tissue were used to measure mitochondrial respiration rates at 37°C using high resolution respirometry (Oroboros Oxygraph 2K, Oroboros Instruments, Innsbruck ,Austria), as previously described for other tissues (12). A multisubstrate protocol was used to sequentially explore the various components of mitochondrial respiratory capacity. To measure the respiration due to oxidative phosphorylation, we added substrates for the activation of specific complexes. Thus, oxygen flux due to complex I activity (Complex I) was quantified by the addition of ADP (5 mM) to a mixture of malate (2mM), pyruvate (10mM) and glutamate (20mM), followed by the addition of succinate (10 mM) to subsequently stimulate complex II (Complex I + II). We then uncoupled respiration to examine the maximal capacity of the electron transport system (ETS) using the protonophore, carbonylcyanide 4 (trifluoromethoxy) phenylhydrazone (FCCP; successive titrations of 0.2 µM until maximal respiration rates were reached). We then examined consumption in the uncoupled state due solely to the activity of complex II by inhibiting complex I with the addition of rotenone (0.1µM; ETS CII). Finally, electron transport through complex III was inhibited by adding antimycin (2 µM) to obtain the level of residual oxygen consumption (ROX) due to oxidating side reactions outside of mitochondrial respiration. The O_2 flux obtained in each step of the protocol was normalized by the wet weight of the tissue sample used for the analysis and corrected for ROX. All respiration experiments comprise 2-3 counterbalanced blocks across days.

Quantification of ATP. Animals were characterized for anxiety and sacrificed under basal conditions by rapid decapitation. The NAc was dissected out and placed in 2 mL of relaxing solution (2.8 mM Ca_2K_2EGTA, 7.2 mM K_2EGTA, 5.8 mM ATP, 6.6 mM $MgCl_2$, 20 mM taurine, 15 mM sodium phosphocreatine, 20 mM imidazole, 0.5 mM dithiothreitol and 50 mM MES, pH = 7.1) until further processing. Tissue samples were then diluted 10x in a tricine buffer solution (40 mM Tricine, 3 mM EDTA, 85 mM NaCl, 3.6 mM KCl, 100 mM NaF and 0.1% saponin, pH 7.4; Sigma Aldrich). ATP content was determined enzymatically with luciferase in a 96-well plate. In the presence of ATP, Mg^{2+} and oxygen, luciferin is oxygenated by luciferase into oxyluciferin. This

reaction emits light which is proportional to the amount of ATP in the sample. ATP was measured with the CellTiter-Glo Luminescent Cell Viability Assay (Promega), with a few minor modifications. A converting solution (100 mM Tricine, 100 mM MgSO4, 25 mM KCl) was added to tissue samples and allowed to incubate at room temperature for 5 min. After incubation, a MgCl2 solution (4 mM tricine and 100 mM MgCl2) was added to the samples, followed by, 100 µl of CellTiter-Glo reagent (G7571, Promega). Additionally, each 96-well plate contained a series of 10-fold dilutions (1µM – 10nM) of an ATP standard (Sigma), in order to generate a standard curve for each assay. Luminescence was immediately detected with a luminometer (Safire 2, Tecan). Luminescence was measured kinetically via 30 samples taken at 1 min intervals. At least 4 points at the plateau were taken to generate an average maximum luminescence for each sample. ATP was calculated using the standard curve to determine the concentration of ATP.

Quantification of lipid peroxidation product 4-HNE. Animals were characterized for anxiety and either sacrificed under basal conditions by rapid decapitation or infused with 10µM mitoQ in the NAc and sacrificed 3 h afterwards. The brain was extracted, frozen at -30°C in isopentane and stored at -80°C until further processing. In basal samples, NAc punches were obtained using on a freezing cryostat and then processed for 4-HNE accumulation using a 4-HNE ELISA assay (Cell BioLabs, Cat.No. STA-334 and STA-838) according to manufacturer's instructions. Samples receiving mitoQ were rapidly fresh-dissected for the NAc and then processed for 4-HNE accumulation as described above.

Isolation of synaptoneurosomal- and glial-enriched fractions. To separate synaptoneurosomes from glial cells, we followed procedures for separation via percoll gradient detailed in (13). Briefly, rats were sacrificed under basal conditions by rapid decapitation and nucleus accumbens from 3 animals per group per experiment were pooled together, rapidly dissected out, and immediately homogenized in a glass tissue grinder in homogenization buffer (1.28M sucrose, 4mM EDTA, 20mM Tris, 50mM DTT, pH 7.4) by 10 even strokes. The homogenate was centrifuged at 1,000*g* for 10 min at 4°C. The supernatant was collected and carefully loaded onto a prepared percoll gradient column (consisting of layers 3, 10, 15, and 23% percoll) and then centrifuged at 31,000*g* for 5 min. at speed at 4°C. Individual synaptoneurosomal- and glial-enriched fractions were then carefully collected from each corresponding percoll layer and protein concentration was determined using the Bradford assay. Both fractions were then washed with ice-cold sucrose/EDTA buffer and centrifuged at 15,000*g* for 15 min. As these two fractions were separated for their subsequent inclusion in respiration analyses, the obtained pellets were resuspended in Mir05 solution and immediately placed inside the Oroboros chambers for respirometry measurements. Five µg of each fraction were reserved and directly loaded onto a 12.5% (w/v) SDS-PAGE for western blot analysis against mouse anti-NeuN (a neuronal marker; Millipore MAB377, 1:1,000), mouse anti-S100 (astrocytic marker; Abcam, ab4066, 1:100), and mouse anti-GAPDH (loading control, Abcam, ab8245, 1:30,000) in order to ensure successful cell separation (see methods Western Blots).

Histology. Animals were bilaterally implanted with cannulae aimed at the NAc, as described above. They received one unilateral infusion (25 ng/ 0.3 µl) of either rotenone, malonic acid, or 3-nitropropionic acid (3NP), with the opposing side receiving the corresponding vehicle (DMSO for rotenone and saline for malonic acid and 3NP treatments). Animals were sacrificed at 24h by pentobarbital injection followed by transcardial perfusion of 0.9% saline solution and paraformaldehyde 4% in PBS (pH=7.5).

H-E staining For hemotoxylin-eosin (HE) staining, brains were dehydrated using increasing steps of EtOH and embedded in paraffin. Sections were cut (10 µm), fixed in acetone for 10 min, and rinsed in distilled water. Sections were incubated with hemotoxylin for 5 min, gently rinsed in tap water for 10 min, and stained in eosin for 2 min. Sections were rinsed in distilled water, dehydrated, and mounted. Images were captured using a brightfield slide scanner (Olympus Slide Scanner VS120-L100).

Cleaved caspase 3 For cleaved caspase 3 analysis, brains were removed, post-fixed for 4 h in 4% paraformaldehyde/PBS and cryoprotected in 30% sucrose/PBS. Coronal sections (30 µm thick) were cut, and free-floating sections were then labeled with a primary antibody against cleaved-caspase 3. Briefly, the floating sections were rinsed with Tris-buffered saline/0.1% Triton-X-100 (TBS-T), and endogenous peroxidases were blocked by incubation in 0.3% H2O2/TBS-T. After washing, sections were blocked in 5% normal donkey serum/TBS-T and incubated overnight at 4°C with antibodies against rabbit anti-cleaved caspase 3 (Cell Signaling, 9661s, 1:400). The sections were washed in TBS-T and incubated for 1 h at room temperature with biotinylated goat anti-rabbit IgG (both 1:200; Vector Laboratories). Images were scanned using a brightfield slide scanner at 20x magnification (Olympus Slide Scanner VS120-L100) and converted to tiff images using the VSI reader actionbar for ImageJ. Images were adsorbed, regions of interest at the site of drug infusion were drawn, and light intensity was measured. At least two sections from each animal were measured and averaged to generate one value per hemisphere per animal for each drug infusion.

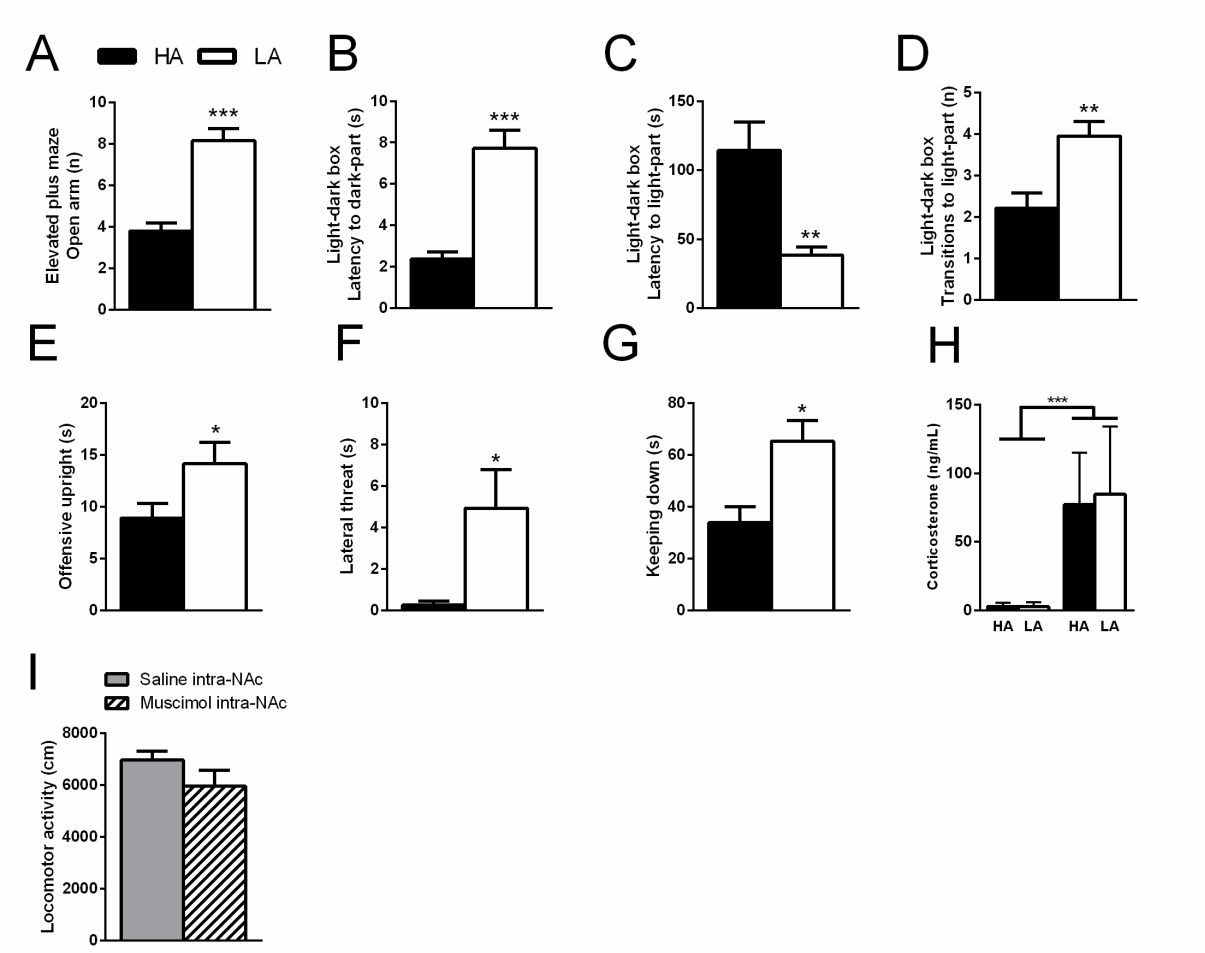

Fig. S1. Characterization of high-anxious and low-anxious rats**.** Rats exhibiting a high- (HA) or low-anxiety (LA) profile based on time spent on the open arms of the elevated plus maze (EPM) also differed in the number of open arm entries on the EPM (**A**). In the light-dark box, high-anxious rats differed from low-anxious rats on all relevant parameters in the expected direction; a reduced latency to enter the lit compartment (**B**), an increased latency to enter the lit compartment (**C**) and reduced number of total dark-light transitions (**D**), *n*= 22-24/group. During social competition, HA rats displayed a reduced duration of behaviors associated with social dominance: offensive upright (**E**), lateral threat (**F**) and keeping down (**G**), *n*= 24/group. Following social competition, corticosterone levels were significantly increased compared to home cage controls, though at both time points, HA and LA rats exhibit similar corticosterone levels (**H**), *n*= 10-20/group. Intra-NAc muscimol did not affect locomotor activity in the open field (**I**), *n*= 8/group. Data are presented as mean ± SEM (*p<0.05, **p<0.01; ***p<0.001, Student's t-test).

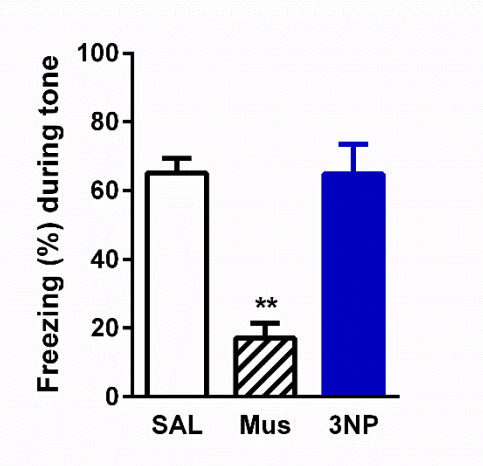

Fig. S2. Acoustic fear conditioning is unaffected by the infusion of the complex II non-competitive inhibitor 3-nitroproprionic acid (3NP) into the basolateral amygdala (BLA). Whereas, intra-BLA infusion of muscimol (Mus; *n*= 4) before training in the acoustic fear conditioning task markedly reduced freezing in response to a tone during the testing session, administration of 3NP (*n*= 8) had no effect on freezing at testing, as compared to saline (SAL; *n*= 5) controls. Data are presented as mean ± SEM (**p<0.01; one-way ANOVA, bonferroni post-hoc comparisons).

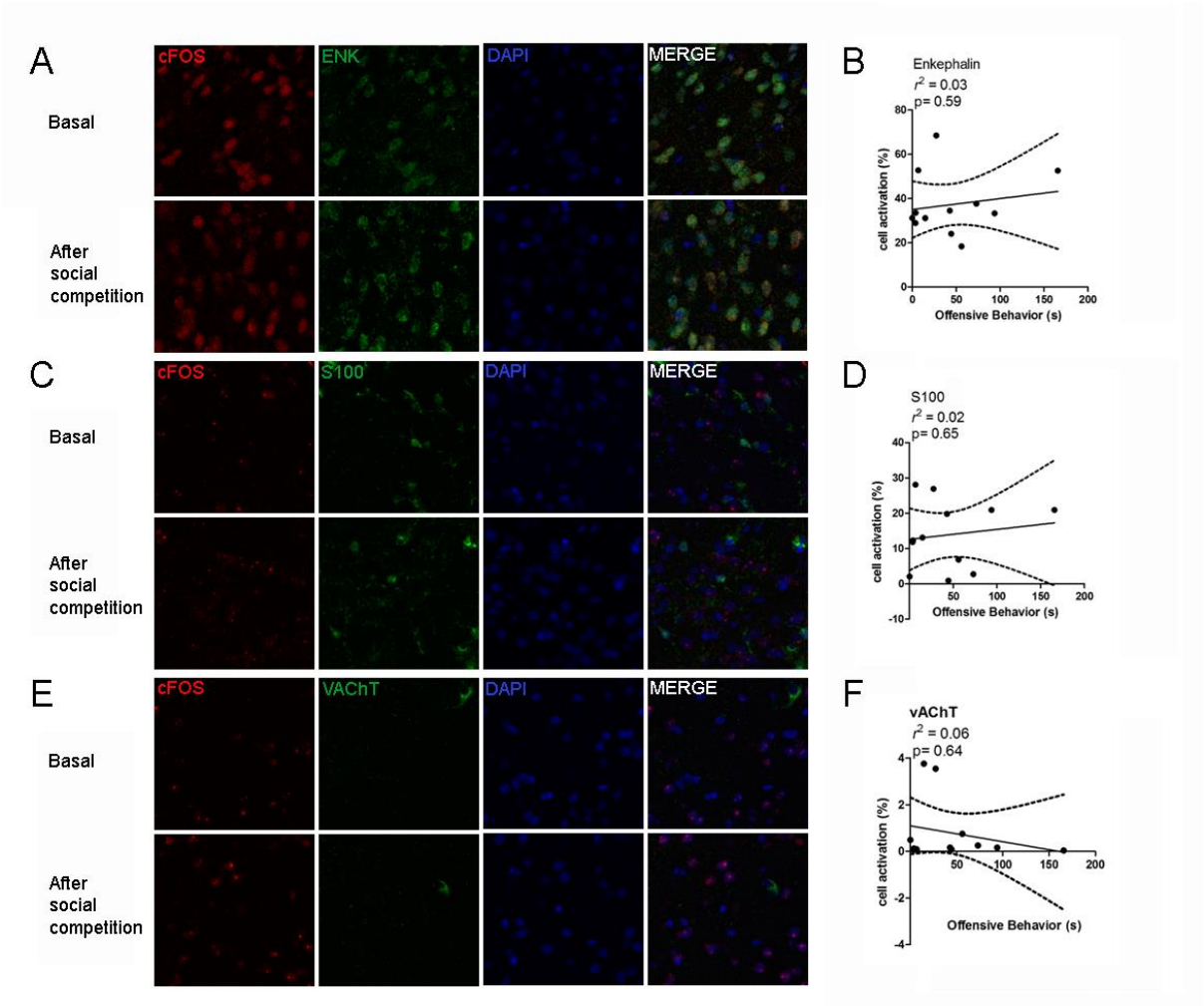

Fig.S3. Representative images of enkephalin (ENK, for D2-containing cells; **A**), S100 (for astrocytic cells; **C**), and vesicular acetylcholine transporter (VAChT, for cholinergic cells; **E**) under basal conditions and following social competition. Double-labeling with cFOS found that neither ENK, S100, nor VAChT correlate significantly with the amount of offensive behavior (**B, D, F**).

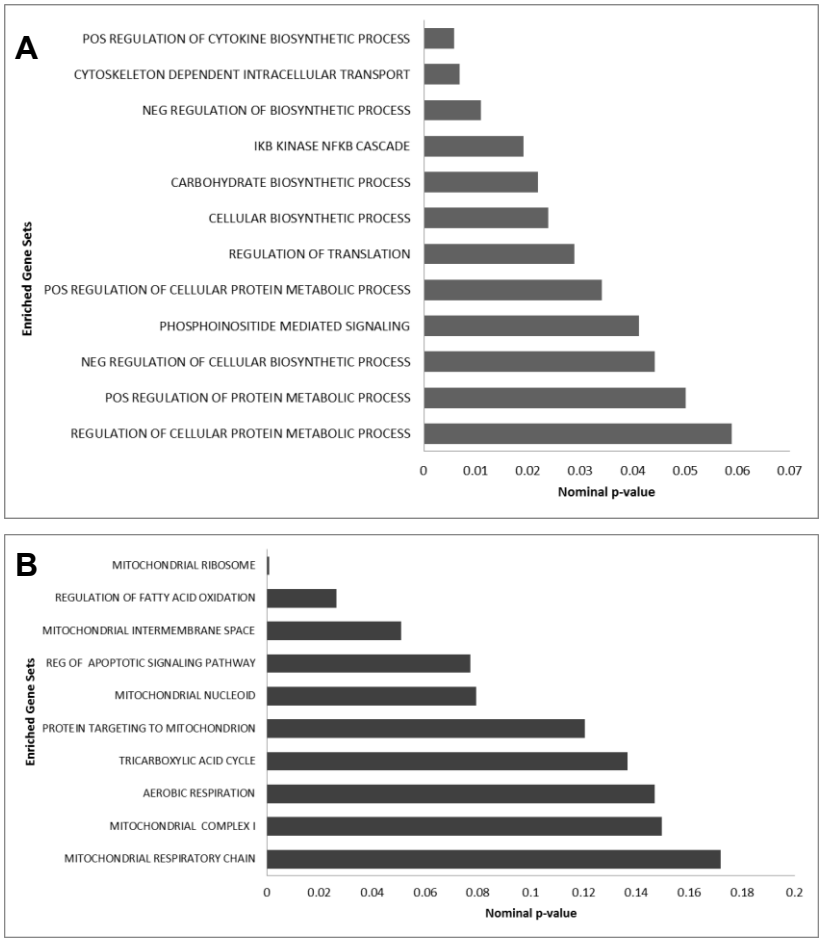

Fig. S4. Gene enrichment analysis indicates a pattern of differential gene expression for metabolic processes and functions within the NAc between high- and low-anxious rats. Gene expression microarrays on high- and low-anxious rats under basal conditions (*n*= 5/group) were performed and analyzed for enrichment using Gene Set Enrichment Analysis (GSEA) software when examining across general GO gene sets (**A**) Enrichment analysis on a curated set of mitochondrial genes identified significantly enriched gene sets related to mitochondrial organization and function (**B**).

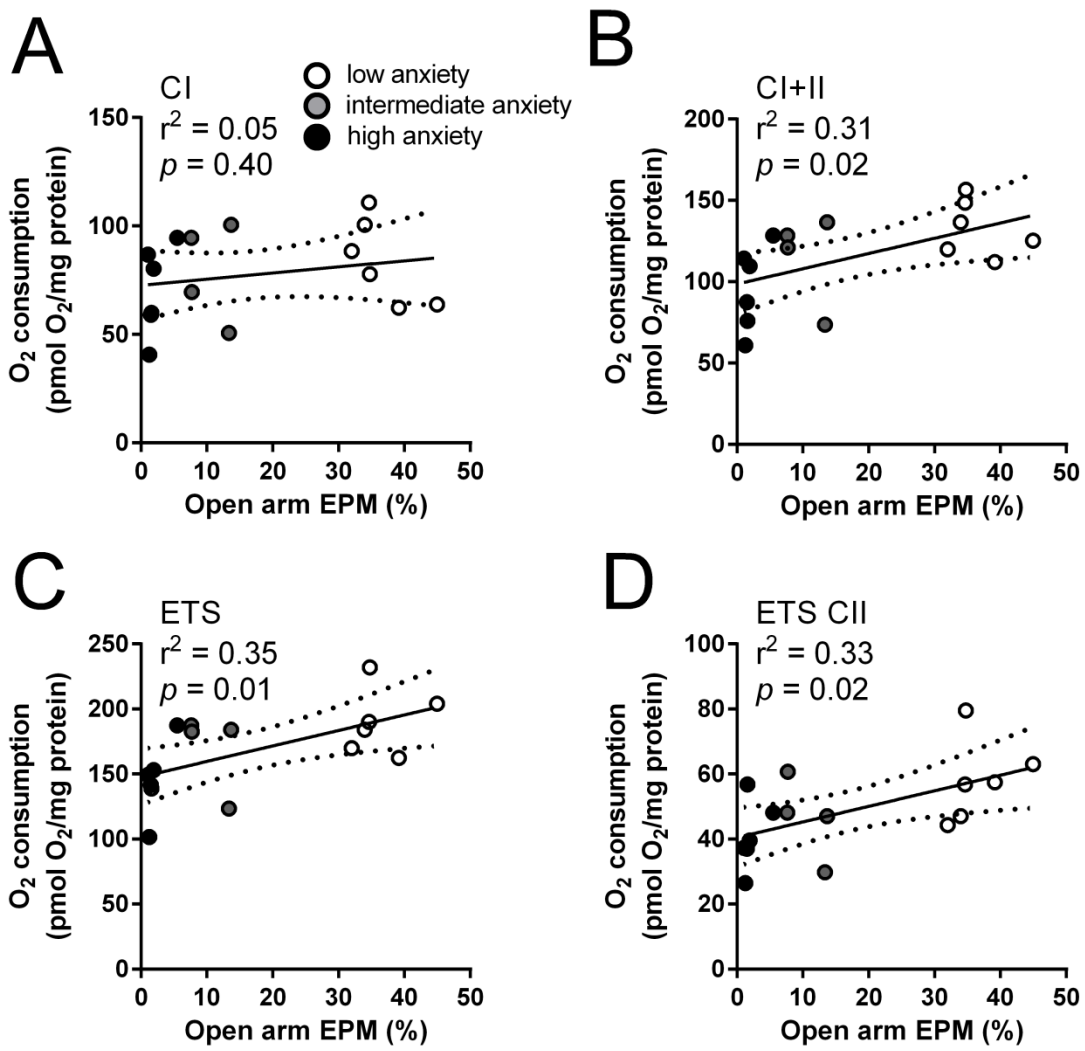

Fig. S5. Correlations between anxiety-like behavior on the elevated plus maze and oxygen consumption for (**A**) stimulation of complex I (CI) by addition of ADP; (**B**) stimulation of complex II (CII) by addition of succinate; (**C**) maximal electron transport system capacity (ETS) by addition of FCCP; and (**D**) maximal capacity due only to complex II (ETS CII) by addition of rotenone. Coefficient of determination (r^2) and p-values calculated from linear regressions.

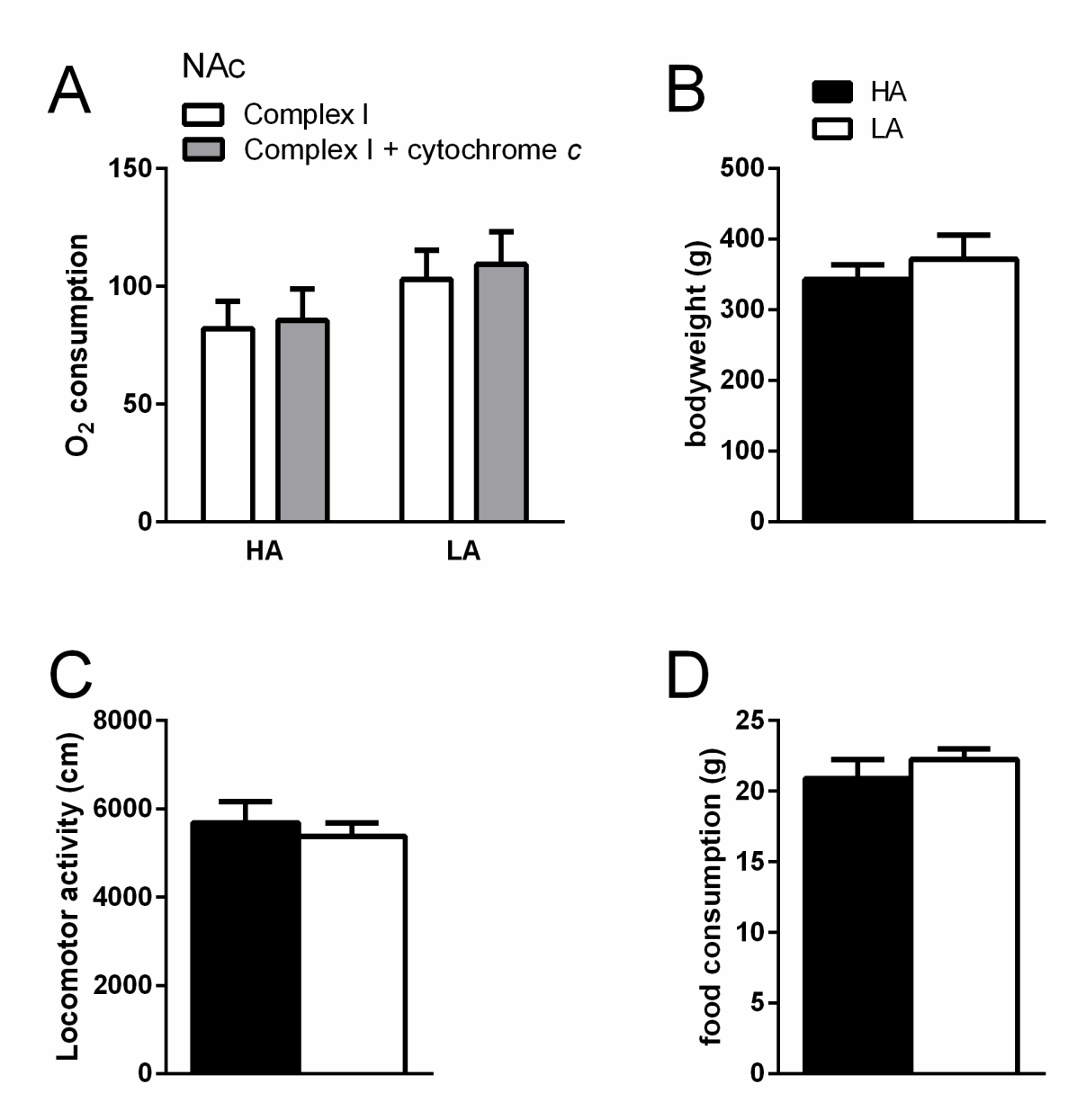

Fig. S6. The difference in mitochondrial respiration between high-anxious (HA) and low-anxious (LA) rats was not the result of differential mitochondrial vulnerability. When mitochondria are damaged, the addition of cytochrome c will replace what had leaked out and therefore enhance respiration. Here, we show that both HA and LA homogenates are unaffected by the addition of 10µM cytochrome c, indicating no differential damage upon processing (**A**). Data are presented as estimated marginal means ± SEM of oxygen flux per mg tissue using a two-way repeated-measures Linear Mixed Model, n=8/group. Differences in trait anxiety respiration were not related to differences in adult body weight (**B**), locomotor activity in the open field (**C**) or overnight food intake (**D**), *n*= 7-11/group.

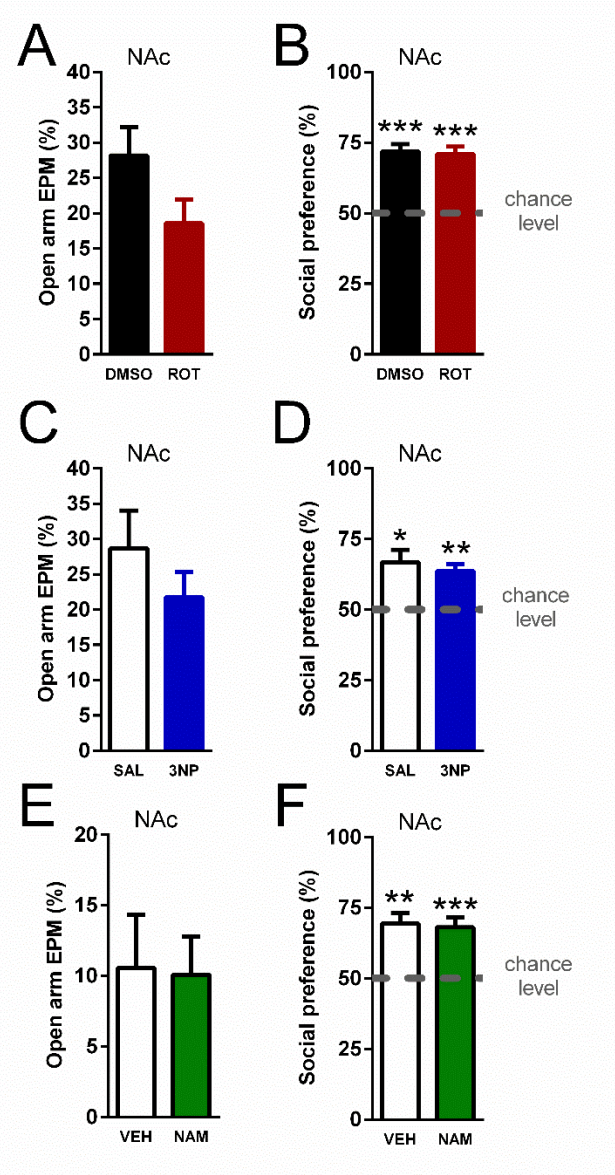

Fig. S7. No effect of mitochondrial treatment on anxiety and social preference. Intra-NAc infusion of rotenone (ROT) had no effect on anxiety (**A**) or social preference (**B**). Infusion of 3-nitroproprionic acid (3NP) similarly did not affect anxiety (**C**) or social preference (**D**). Intra-NAc infusion of nicotinamide (NAM) also did not affect anxiety (**E**) or social preference (**F**), *n*= 9-12/group. Data are presented as mean ± SEM (**p<0.01, ***p<0.001, Student's t-test or one-sample t-test against chance- level).

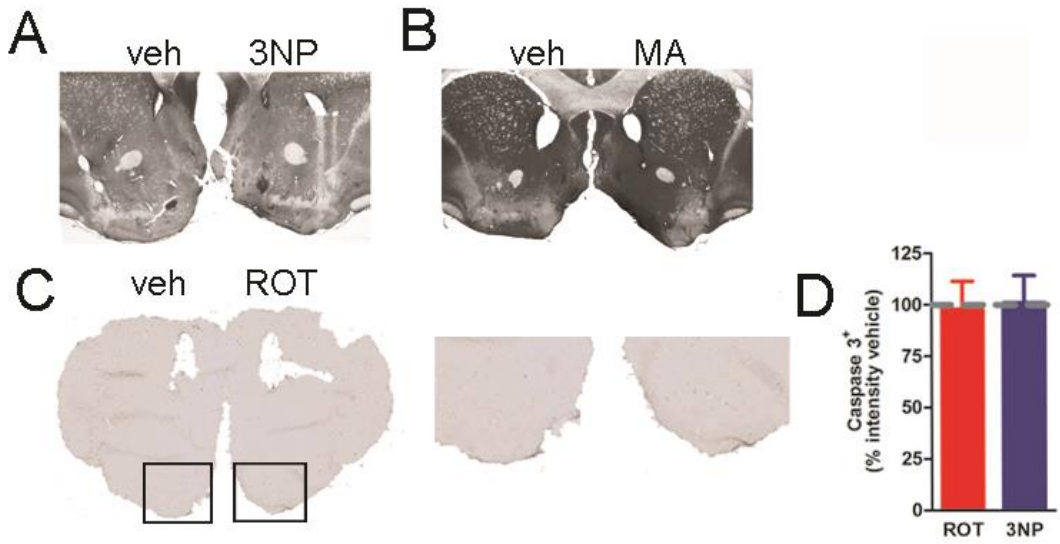

Fig. S8. The intra-NAc infusion of malonic acid (MA) or 3-nitroproprionic acid (3NP) at the dosing scheme used in the current study (25ng/hemisphere, 10 min prior to behavioral testing) did not affect gross brain morphology as shown by HE-staining (**A,B**). Nor were there effects of the mitochondrial inhibitors on apoptotic cell death (**C-D**) as evidenced by the amount of cleaved-caspase 3. Data (**D**) are represented as mean ± SEM (n= 3/group, Student's t-test).

Supplementary Table 1: Differentially expressed genes between high- and low-anxious rats from curated mitochondrial gene sets

mRNA Accession #	Gene Symbol	Gene Description	GO Accession	GO name	P-Value
NM_001002253	Atp6v0e2	ATPase, H+ transporting V0 subunit e2	> GO:0015991	ATP hydrolysis coupled proton transport	0.005
NM_053994	Pdha2	Pyruvate dehydrogenase (lipoamide) alpha 2	> GO:0004739	Pyruvate dehydrogenase activity	0.006
NM_001108898	Ddx28	DEAD (Asp-Glu-Ala-Asp) box polypeptide 28	> GO:0042645	Mitochondrion nucleoid	0.009
NM_001013431	Chchd4	Coiled-coil-helix-coiled-coil-helix domain containing 4	> GO:0006626	Protein targeting to mitochondria	0.012
NM_053970	Nln	Neurolysin (metallopeptidase M3 family)	> GO:0005739	Mitochondrion	0.031
NM_017254	Htr2a	5-hydroxytryptamine (serotonin) receptor 2A	> GO:0006816	Calcium ion transport	0.031

Table S1. Differentially expressed genes between high- and low-anxious rats identified in the custom-curated mitochondrial gene sets following gene enrichment analysis. P-values were obtained from a general linear model of anxiety and gene expression.

Supplementary Table 2: Mitochondrial density and length in high- and low-anxious rats

Measurement	HA	LA	p-value
Total Density (per μm^2)	0.75±0.05	0.70±0.06	0.53
Density within dendrites (per μm^2)	0.50±0.04	0.50±0.05	0.98
Total Length (μm)	438.3± 17.3	423.5± 25.7	0.66

Table S2. Total mitochondrial density, density within dendrites and total mitochondrial length in the nucleus accumbens measured in images captured by electron microscopy did not differ between high- (HA) and low-anxious (LA) rats. Density is presented as mean mitochondria per μm^2 ± SEM (Student's t-test). Length is presented as mean µm per 1500 mitochondria ± SEM (Student's t-test). In the lower panel, a TEM representative image highlighting mitochondria with internal inserts is shown.

Supplementary Table 3: Effects of anxiety and NAc treatments on other social behaviors

Dyad Composition	Condition	Social Investigation (s)	p-value	Auto-grooming (s)	p-value
HA	Basal	128.3 ± 10.0	0.94	41.1 ± 6.7	0.57
LA	Basal	129.5 ± 12.5		36.2 ± 5.9	
Matched	ROT	156.9 ± 23.0	0.36	87.9 ± 20.6	0.39
	DMSO	129.2 ± 24.2		56.7 ± 20.2	
Matched	MA	122.1 ± 16.5	0.83	46.5 ± 10.6	0.49
	Saline	134.8 ± 18.5		42.8 ± 9.6	
Matched	3NP	161.4 ± 23.4	0.57	51.0 ± 9.6	0.91
	Saline	164.6 ± 21.3		64.8 ± 13.7	
HA	NAM	143.5 ± 29.0	0.47	72.8 ± 17.4	0.89
HA	Saline	118.8 ± 16.4		76.2 ± 23.2	
Matched	MUS	107.5 ± 27.5	0.02	43.7 ± 15.5	0.89
	Saline	211.1 ± 27.5		40.3 ± 16.9	

Table S3. The specificity for each of the pharmacological treatments given intra-NAc on social competition was investigated by measuring the total duration of social investigation and auto-grooming during the social encounter. Dyads consisted of either high- and low-anxious (HA, LA respectively) rats or anxiety-matched rats (Matched). Abbreviations: ROT, rotenone; DMSO, dimethylsulfoxide; 3NP, 3-nitropropionic acid; MA, malonic acid; NAM, nicotinamide; MUS, muscimol. Data are presented as mean ± SEM (Student's t-test).

References:

1. Herrero AI, Sandi C, & Venero C (2006) Individual differences in anxiety trait are related to spatial learning abilities and hippocampal expression of mineralocorticoid receptors. *Neurobiol Learn Mem* 86(2):150-159.
2. Cordero MI & Sandi C (2007) Stress amplifies memory for social hierarchy. *Front Neurosci* 1(1):175-184.
3. Koolhaas JM, Schuurman T, & Wiepkema PR (1980) The organization of intraspecific agonistic behaviour in the rat. *Prog Neurobiol* 15(3):247-268.
4. Hollis F, Gaval-Cruz M, Carrier N, Dietz DM, & Kabbaj M (2012) Juvenile and adult rats differ in cocaine reward and expression of zif268 in the forebrain. *Neuroscience* 200:91-98.
5. Paxinos G & Watson C (2006) *The rat brain in stereotaxic coordinates: hard cover edition* (Academic press).
6. Preibisch S, Saalfeld S, & Tomancak P (2009) Globally optimal stitching of tiled 3D microscopic image acquisitions. *Bioinformatics* 25(11):1463-1465.
7. Irizarry RA*, et al.* (2003) Exploration, normalization, and summaries of high density oligonucleotide array probe level data. *Biostatistics* 4(2):249-264
8. Ritchie ME*, et al.* (2015) limma powers differential expression analyses for RNA-sequencing and microarray studies. *Nucleic Acids Res* 43(7).
9. Gentleman RC*, et al.* (2004) Bioconductor: open software development for computational biology and bioinformatics. *Genome Biol* 5(10):R80.
10. Subramanian A*, et al.* (2005) Gene set enrichment analysis: a knowledge-based approach for interpreting genome-wide expression profiles. *Proc Natl Acad Sci USA* 102(43):15545-15550.
11. Cardona A*, et al.* (2012) TrakEM2 software for neural circuit reconstruction. *PLoS One* 7(6):e38011.
12. Holmstrom MH, Iglesias-Gutierrez E, Zierath JR, & Garcia-Roves PM (2012) Tissue-specific control of mitochondrial respiration in obesity-related insulin resistance and diabetes. *Am J Physiol Endocrinol Metab* 302(6):E731-739.
13. Dunkley PR, Jarvie PE, & Robinson PJ (2008) A rapid Percoll gradient procedure for preparation of synaptosomes. *Nat Protoc* 3(11):1718-1728.